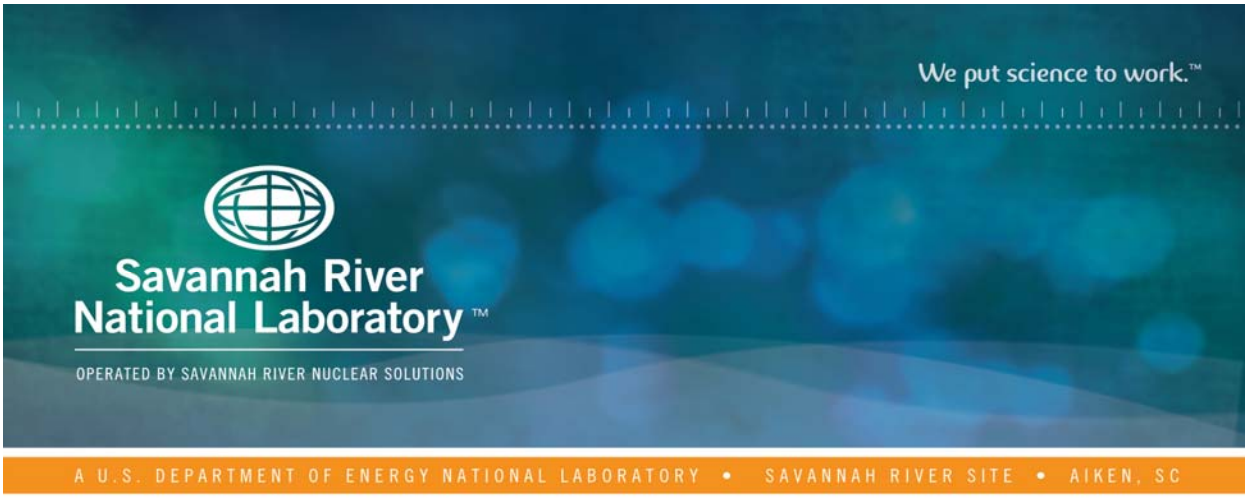

AFS-2 Flowsheet Modifications to Address the Ingrowth of Pu(VI) during Metal Dissolution

Kimberly P. Crapse
Tracy S. Rudisill
Patrick E. O'Rourke
Edward A. Kyser, III

July 2014
SRNL-STI-2013-00709, Revision 0

DISCLAIMER

Printed in the United States of America

Prepared for
U.S. Department of Energy

SRNL-STI-2013-00709
Revision 0

Keywords: *Plutonium Metal, H Canyon, Dissolution, Valence, Oxidation State*

Retention: *Permanent*

AFS-2 Flowsheet Modifications to Address the Ingrowth of Pu(VI) during Metal Dissolution

Kimberly P. Crapse
Tracy S. Rudisill
Patrick E. O'Rourke
Edward A. Kyser, III

July 2014

Prepared for the U.S. Department of Energy under contract number DE-AC09-08SR22470.

Savannah River National Laboratory™
OPERATED BY SAVANNAH RIVER NUCLEAR SOLUTIONS

REVIEWS AND APPROVALS

AUTHORS:

_____
Kimberly P. Crapse, Separations and Actinide Science Programs Date

_____
Tracy S. Rudisill, Separations and Actinide Science Programs Date

_____
Patrick E. O'Rourke, Office of Analytical Science Date

_____
Edward A. Kyser, III, Separations and Actinide Science Programs Date

TECHNICAL REVIEW:

_____
Jonathan M. Duffey, Separations and Actinide Science Programs Date

_____
Kathryn M. Taylor-Pashow, Separations and Actinide Science Programs Date

_____
Robert J. Lascola, Jr., Analytical R & D Programs Date

_____
W. H. Clifton, Jr., H Canyon Engineering Date

APPROVAL:

_____
Timothy B. Brown, Manager Date
Separations and Actinide Science Programs

_____
S. L. Marra, Manager Date
Environmental & Chemical Process Technology Research Programs

_____
K. J. Usher, Manager Date
H Canyon Engineering

EXECUTIVE SUMMARY

In support of the Alternate Feed Stock Two (AFS-2) PuO_2 production campaign, Savannah River National Laboratory (SRNL) conducted a series of experiments concluding that dissolving Pu metal at 95 °C using a 6–10 M HNO_3 solution containing 0.05–0.2 M KF and 0–2 g/L B could reduce the oxidation of Pu(IV) to Pu(VI) as compared to dissolving Pu metal under the same conditions but at or near the boiling temperature. This flowsheet was demonstrated by conducting Pu metal dissolutions at 95 °C to ensure that PuO_2 solids were not formed during the dissolution. These dissolution parameters can be used for dissolving both Aqueous Polishing (AP) and MOX Process (MP) specification materials.

Preceding the studies reported herein, two batches of Pu metal were dissolved in the H-Canyon 6.1D dissolver to prepare feed solution for the AFS-2 PuO_2 production campaign. While in storage, UV-visible spectra obtained from an at-line spectrophotometer indicated the presence of Pu(VI). Analysis of the solutions also showed the presence of Fe, Ni, and Cr. Oxidation of Pu(IV) produced during metal dissolution to Pu(VI) is a concern for anion exchange purification. Anion exchange requires Pu in the +4 oxidation state for formation of the anionic plutonium(IV) hexanitrato complex which absorbs onto the resin. The presence of Pu(VI) in the anion feed solution would require a valence adjustment step to prevent losses. In addition, the presence of Cr(VI) would result in absorption of chromate ion onto the resin and could limit the purification of Pu from Cr which may challenge the purity specification of the final PuO_2 product.

Initial experiments were performed to quantify the rate of oxidation of Pu(IV) to Pu(VI) (presumed to be facilitated by Cr(VI)) as functions of the HNO_3 concentration and temperature in simulated dissolution solutions containing Cr, Fe, and Ni. In these simulated Pu dissolutions studies, lowering the temperature from near boiling to 95 °C reduced the oxidation rate of Pu(IV) to Pu(VI). For 8.1 M HNO_3 simulated dissolution solutions, at near boiling conditions >35% Pu(VI) was present in 50 h while at 95 °C <10% Pu(VI) was present at 50 h. At near boiling temperatures, eliminating the presence of Cr and varying the HNO_3 concentration in the range of 7–8.5 M had little effect on the rate of conversion of Pu(IV) to Pu(VI). HNO_3 oxidation of Pu(IV) to Pu(VI) in a pure solution has been reported previously[1].

Based on simulated dissolution experiments, this study concluded that dissolving Pu metal at 95 °C using a 6 to 10 M HNO_3 solution 0.05–0.2 M KF and 0–2 g/L B could reduce the rate of oxidation of Pu(IV) to Pu(VI) as compared to near boiling conditions. To demonstrate this flowsheet, two small-scale experiments were performed dissolving Pu metal up to 6.75 g/L. No Pu-containing residues were observed in the solutions after cooling. Using Pu metal dissolution rates measured during the experiments and a correlation developed by Holcomb [2], the time required to completely dissolve a batch of Pu metal in an H-Canyon dissolver using this flowsheet was estimated to require nearly 5 days (120 h). This value is reasonably consistent with an estimate based on the Batch 2 and 3 dissolution times in the 6.1D dissolver and Pu metal dissolution rates measured in this study and by Rudisill et al. [3]. Data from the present and previous studies show that the Pu metal dissolution rate decreases by a factor of approximately two when the temperature decreased from boiling (112 to 116 °C) to 95 °C. Therefore, the time required to dissolve a batch of Pu metal in an H-Canyon dissolver at 95 °C would likely double (from 36 to 54 h) and require 72 to 108 h depending on the surface area of the Pu metal.

Based on the experimental studies, a Pu metal dissolution flowsheet utilizing 6–10 M HNO_3 containing 0.05–0.2 M KF (with 0–2 g/L B) at 95 °C is recommended to reduce the oxidation of Pu(IV) to Pu(VI) as compared to near boiling conditions. The time required to completely dissolve a batch of Pu metal will increase, however, by approximately a factor of two as compared to initial dissolutions at near boiling (assuming the KF concentration is maintained at nominally 0.1 M). By lowering the temperature to 95 °C under otherwise the same operating parameters as previous dissolutions, the Pu(VI) concentration should

not exceed 15% after a 120 h heating cycle. Increasing the HNO_3 concentration and lowering Pu concentration are expected to further limit the amount of Pu(VI) formed.

TABLE OF CONTENTS

LIST OF TABLES

LIST OF FIGURES

LIST OF ABBREVIATIONS

AFS-2	Alternate Feed Stock Two
AP	Aqueous Polishing
GPHA	Gamma Pulse Height Analysis
ICP-ES	Inductively Coupled Plasma Emission Spectroscopy
MOX	Mixed Oxide Fuel
MP	MOX process
NIR	Near infrared
PCR	Principal Component Regression
SRNL	Savannah River National Laboratory

1.0 Introduction

Two batches of Pu metal were dissolved in the H-Canyon 6.1 D dissolver to prepare feed solution for the Alternate Feed Stock Two (AFS-2) PuO_2 production campaign. The HB-Line Phase II facility plans to purify Pu and convert it to the oxide. The solution from each batch was first transferred separately to Tank 7.4 and then to Tank 12.2. Subsequently, due to higher than expected ^{242}Pu, both batches were transferred and combined together in Tank 12.1 for storage. The initial batch of metal (sampled in Tank 12.2) was dissolved in nominally 9 M HNO_3 containing 0.05 M fluoride. The total dissolution time was approximately 130 hours. The second batch of metal (sampled in Tank 7.4) was dissolved in nominally 9 M HNO_3 containing 0.1 M fluoride. The total dissolution time was approximately 36 hours. Both batches of solution contain concentrations of Fe from the carbon steel packaging cans and dissolver insert end caps, corrosion products from the dissolver (i.e., Fe, Ni, and Cr), and boric acid (0.1–0.2 M) added as a neutron poison [4].

While in storage, UV-visible spectra of the Tank 12.2 initial batch solution obtained from an at-line spectrophotometer indicated the presence of Pu(VI). Analysis of the solutions also showed Fe, Ni, and Cr. Oxidation of Pu(IV) to Pu(VI) during metal dissolution is a concern for anion exchange purification. Anion exchange requires Pu in the Pu(IV) oxidation state for formation of the anionic plutonium hexanitrato complex which absorbs onto the resin. The presence of Pu(VI) in the anion feed solution would require a valence adjustment step to prevent losses. In addition, the presence of Cr(VI) would result in absorption of chromate ion onto the resin and could limit the purification of Pu from Cr which may challenge the purity specification of the final PuO_2 product. Samples from Tank 12.2 (batch 1) and Tank 7.4 (batch 2) were analyzed at SRNL for the Pu(VI) content by UV-visible spectroscopy along with prepared Pu(IV) and Pu(VI) reference standards. Kyser estimated that these samples contained 1–3 g Pu(VI)/L [4] and minimal amounts of Cr(VI) [5].

The dissolution of Pu metal in 8–10 M HNO_3 containing 0.05–0.2 M KF and 0–2 g/L B [3] results in the corrosion of the 304L stainless steel dissolver vessel. The corrosion rate depends on the temperature, time at temperature, and concentrations of HNO_3, free fluoride, and other cations in the dissolving solution which complex fluoride (e.g., B, Fe, Ni, Cr, and Pu). In HNO_3 solution, the expected oxidation states of the metals are Fe(III), Cr(III), Ni(II), and Pu(IV). Since Fe(III) and Ni(II) are present in their most stable oxidation states (in HNO_3), subsequent oxidation-reduction reactions are not expected; however, both Cr(III) and Pu(IV) are subject to oxidation under conditions present in the dissolver. In hot HNO_3, oxidation of Cr(III) to Cr(VI) will occur. Smith and Purdy [4] measured the Cr(III) oxidation rate in boiling HNO_3 at concentrations ranging from 7.7–15.4 M. In 7.7 M HNO_3, the rate of oxidation was negligible. In 10 M acid, there appeared to be a 4–5 hour induction period before oxidation initiated. In concentrated acid, the induction period was negligible and the oxidation proceeded immediately.

There is limited available information in the literature on the oxidation of Pu(IV) by Cr(VI). Cr(VI) is a powerful oxidizing agent, which undergoes reduction back to Cr(III) by reaction with any oxidizable species in solution. The formation of Cr(VI) will accelerate the corrosion of the dissolver by oxidizing the metals in the stainless steel alloy [6]. The oxidation of Pu(IV) due to the presence of Cr(VI) will also occur [6]. Newton and Burkhart [7] reported the preparation of a Cr(III)–Pu(V) complex by the oxidation of Pu(IV) using Cr(VI). In this work the authors found that Pu(IV) oxidation was moderately rapid when the Pu was combined with excess Cr(VI) in $HClO_4$. However, only about half the total Pu(IV) was oxidized directly to Pu(VI). Several days were required before all of the Pu was converted. The Pu which was not converted was present

as the Cr(III)–Pu(V) complex which was stable enough for recovery by ion exchange. Posvol'skii and Tsirlin [8] reported that the oxidation of Pu(IV) by Cr(VI) proceeds extremely slowly at low temperatures (i.e., <50 °C). The authors also describe the induced oxidation of Pu(IV) by Cr(VI) in which a reducing agent (e.g., nitrous acid and Fe(II)) forms an intermediate complex with the reactants which accelerates the oxidation [8]. In subsequent work, the authors reported the catalytic effect of several metals (e.g., Fe(III), Mn(II), and Ni(II)) on the induced oxidation of Pu(IV) by Cr(VI). The results were mixed, with various metals showing positive, negative, and no catalytic effect on the oxidation rate [9].

1.1 Objectives

The purpose of the experimental work described in this report was two-fold. Initial experiments were performed to quantify the rate of oxidation of Pu(IV) to Pu(VI) (presumed to be facilitated by Cr(VI)) as functions of the HNO_3 concentration and temperature to identify dissolution conditions which minimized the production of Pu(VI). In these simulated dissolution experiments, concentrations of Pu, Fe, Ni, and Cr which were representative of the concentrations in Tank 7.4 (i.e., batch 2) were added to 6–8.4 M HNO_3 solutions containing 0.1 M KF and 1.3 g/L B. The solutions were heated to temperatures ranging from 95 °C to the boiling point for 50 to 100 hours. Periodically, samples of solution were removed from the reaction vessel and the UV–visible spectrum recorded to quantify the amount of Pu(IV) which had oxidized to Pu(VI).

Based on the simulated dissolution experiments, this study concluded that dissolving Pu metal at 95 °C using a 6 to 10 M HNO_3 solution containing 0.1 M KF and 0–2 g/L B could reduce the oxidation of Pu(IV) to Pu(VI). To demonstrate this flowsheet, two Pu metal dissolution experiments (one with B present for AP specification material and one without B for MP specification material) were performed to ensure that the metal would completely dissolve without the generation of PuO_2 solids. During the experiments, the Pu metal was periodically removed from the dissolving vessel to measure the mass and surface area to permit the calculation of the dissolution rate. At these times, samples of the dissolving solution were also removed to measure the Pu(VI) concentration by UV-visible spectroscopy and total Pu by gamma pulse height analysis (GPHA). Hydrogen generation was not measured in these Pu metal dissolution experiments but has been addressed in detail in previous studies [3]. The experimental methods used to perform the simulated dissolution experiments and the flowsheet demonstrations and a discussion of the results are presented in the following sections.

2.0 Experimental Procedure

2.1 Simulated Metal Dissolutions

2.1.1 *Test Matrix*

In order to determine the key variables controlling conversion of Pu(IV) to Pu(VI) under H-Canyon dissolver conditions, multiple experiments were carried out to differentiate the contributions of HNO_3 concentration, Cr (added as Cr(III)), and temperature to the rate of conversion of Pu(IV) to Pu(VI) in nitric acid solutions. The concentration of Pu(IV) is an additional factor affecting the rate of Pu(VI) ingrowth [1]. Pu concentration was not specifically targeted in this study.

Target concentrations for a series of seven tests simulating H-Canyon dissolving solutions are presented in Table 2-1. Tests 0–6 were designed to match known Tank 7.4 measured concentrations of B, Fe, Cr, and Ni [1]. HNO_3 molarities (Tests 0–5; Table 2-1) were calculated based on HNO_3 added using an assumed HNO_3 molarity for the Pu stock solution (which was the same for Tests 0–5). Test 6 was a 100-mL aliquot of the final solution from the Pu metal dissolution experiment M1 described in detail in Section 2.2. The metal dissolution experiment was performed at 95 °C, cooled, and stored for several weeks prior to Test 6 (see Sections 2.2 and 3.2). Tests 0–5 did not contain Pu(VI) in the initial solution. The UV-vis spectra of the initial Test 6 solution indicated a small amount of Pu(VI) (0.70 g/L) was initially present before heating (as a result of the original Pu metal dissolution, cooling, and storage). Due to the short duration of the M1 dissolution test, Test 6 was carried out to determine the rate of Pu(VI) ingrowth during prolonged heating at 95 °C which is more representative of the time required to dissolve a batch of Pu metal in an H-Canyon dissolver. Measured values of the solution components for Test 1–6 can be found in Appendix A (Table A-2 through Table A-4)

Table 2-1. Target Concentration in Simulated Pu Dissolving Solutions

Component	Test 0	Test 1	Test 2	Test 3	Test 4	Test 5	Test 6
Material Type	7.4	7.4	7.4	7.4	7.4	7.4	M1
HNO_3 (M)	8.4	8.1	7.0	8.1	8.1	8.1	6.0
Pu (g/L)	3.81	3.51	3.51	3.51	3.78	3.51	6.75
KF (M)	0.1	0.1	0.1	0.1	0.1	0.1	0.1
B (g/L)	1.3	1.5	1.5	1.5	1.5	1.5	1
Fe (g/L)	3.6	3.5	3.5	3.5	3.5	3.5	3.5
Cr (g/L)	0.67	0.61	0.61	0	0.60	0.61	0.61
Ni (g/L)	0	0.38	0.38	0.38	0.37	0.38	0.37

Target temperatures for Tests 0–6 are presented in Table 2-2. In Tests 0–3 and Test 6 the temperature was constant throughout the experiment with Tests 0–3 targeting near boiling conditions. In Tests 4 and 5, the temperature was heated initially to 95 °C for an extended period of time before successively increasing the temperature to 100 °C and 105 °C for extended heating at each temperature.

Table 2-2. Target Temperatures for Simulated Pu Dissolving Solution Experiments

	Test 0	Test 1	Test 2	Test 3	Test 4	Test 5	Test 6
Temperature (°C)	116	110	108	110	95 100 105	95 100 105	95

2.1.2 *Simulated Pu Dissolution Experimental Setup*

The experimental setup consisted of a 125-mL, 4-port boiling flask fitted with a small condenser cooled with once-through process water (Test 0) or process water recirculated using a small peristaltic pump (Tests 1–6) (Figure 2-1a). The flask and condenser were attached to a ringstand on a single-position digital stirring hotplate (Thermo Scientific Super-Nuova™ Single-Position Digital Stirring Hotplates available from Fisher Scientific, model 11-675-917Q). The solution temperature was controlled using a 1/8" K type Teflon coated thermocouple using the external temperature input on the hotplate.

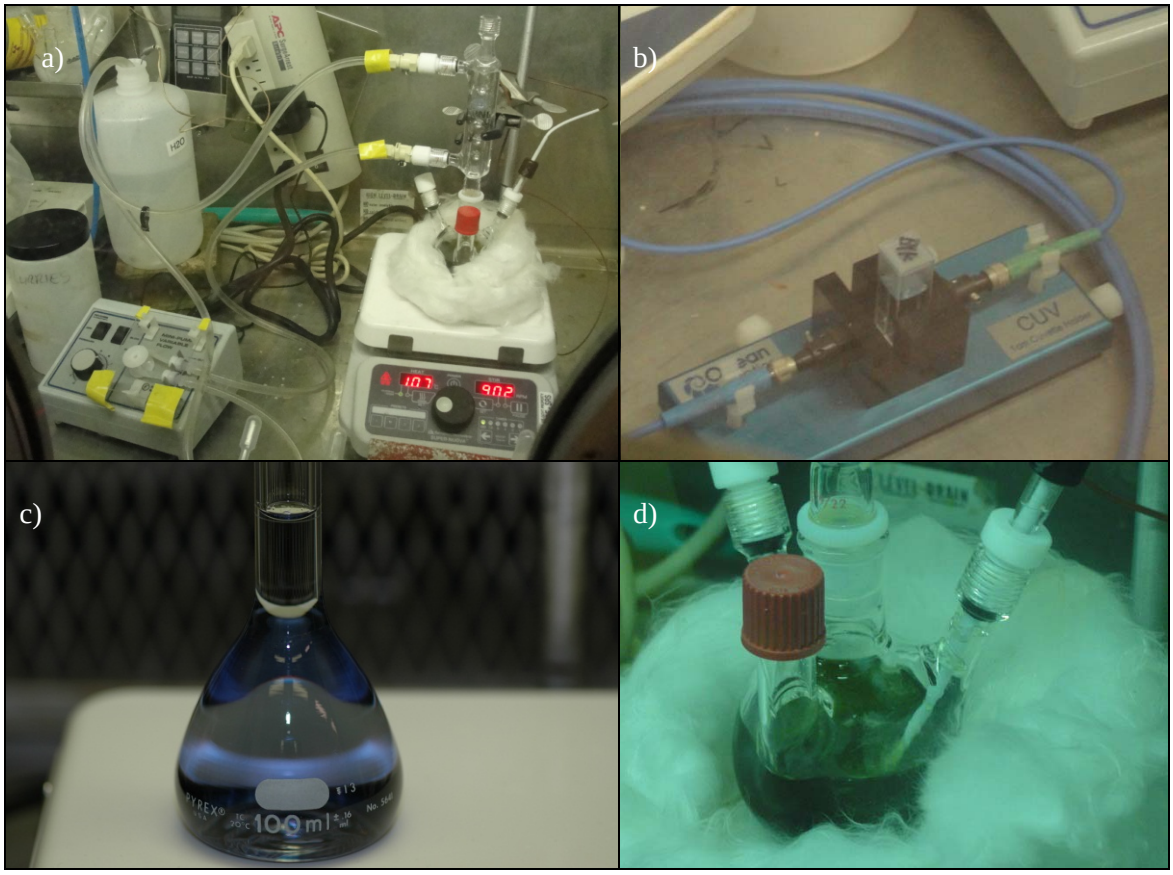

Figure 2-1. a) Experimental setup b) UV-visible spectroscopy fiber optics and cuvette holder. c) Nitric acid stock solution (8 M) with B, F, Fe, Cr, and Ni. d) Simulated Pu dissolving solution.

The solution was prepared stepwise with a goal of simulating Tank 7.4 solution with Cr added as 100% Cr(III) and Pu added as 100% Pu(IV). In a scoping study, Test 0, a stock HNO_3 solution with boric acid and KF was prepared and Pu(IV) stock solution was added to a portion of that solution matrix. Cr(III) and Fe(III) nitrate salts were added after the absence of Pu(VI) was confirmed spectroscopically. The Fe(III) and Cr(III) were added last out of concern that their presence could complicate a valence adjustment step if one had been necessary. For each of the subsequent tests (Tests 1–5), a stock HNO_3 solution with all components except Pu(IV) was prepared (Figure 2-1c). After adding the stock solution of Pu(IV) to this matrix solution, a sample of the initial simulant solution was taken for characterization (UV-visible spectroscopy

(Figure 2-1b), total and free acid, and ICP-ES and Pu analysis by GPHA). Figure 2-1d shows the 8.1 M HNO_3 simulated dissolving solution containing Pu.

Samples from the tests were analyzed using a glovebox setup for UV-visible spectroscopy. A pair of fiber optic cables installed through the ceiling of the glovebox allow a light signal from a tungsten-halogen lamp source to be brought into the glovebox, passed through the cuvette (containing either a reference solution or a sample) (Figure 2-1b), and carried out of the glovebox back to an AvaSpec-2048TEC thermo-electric cooled spectrometer controlled by a computer. Reference and measurement spectra were taken on the same pair of NIR grade fibers. Light references were taken prior to the beginning of the experiment and stored. Absorption spectra were collected using the spectrophotomer with water as a reference solution. Absorption spectral data was collected and saved to computer files using the macro-enabled Excel workbook, Avantes_Model.xlsm which was developed at SRNL to interface with Avantes spectrometer control program Avaspec ver.7.6. The data collected in these experiments was used to build Principal Component Regression (PCR) models which relate features in the UV-visible spectroscopy data to concentration. Data analysis was carried out using Excel macro programs from PCR_Macro_New-B.xlsm, developed at SRNL.

2.1.3 *Analysis of the UV-visible Spectroscopy Data*

Absorption spectra, collected from solutions extracted at various times from the test vessel, were analyzed at ambient temperature to determine Pu(IV) and Pu(VI) concentrations. Total plutonium concentration was assumed to be constant during the course of each test, and the absorption signals from Pu(IV) and Pu(VI) are assumed to respond linearly to the Pu(IV) and Pu(VI) concentrations. Absorption spectral data was mathematically processed to remove baseline offsets and scattering effects by convoluting them with a second derivative Gaussian filter (sigma=2 channels, kernel limits = +/-50 channels). Processed spectra were analyzed using Principal Component Regression. The PCR method constructs artificial principal components (PC's), similar to measured spectra, by using weighted averages of spectra in a data set to describe the maximum amount of signal variance. PCR of the data from each test showed only two significant PC's, assumed to be from Pu(IV) and Pu(VI) species. For Tests 1–5, the full analysis ranges used in the modeling were 425–540 and 775–875 nm. For Test 0 and Test 6, 425–875 nm was used. For Tests 1–5, the analysis was subjected to the constraint that the initial concentration of Pu(VI) = 0 and for Test 6 a small amount of Pu(VI) (0.70 %) was present initially which introduced a small correction to the area minimization analysis. These two PC's from each test were used to derive spectra which correspond to the real components for Pu(VI) and Pu(IV) by a process of selected region minimization described elsewhere [10]. The wavelength region used for the selected area minimization was 800 nm to 845 nm which covers the main Pu(VI) signal area. The derived Pu(VI) and Pu(IV) spectra are the basis for a spectral fitting model to predict the actual Pu(VI) and Pu(IV) concentration in each sample. The fit model from one test cannot be applied to a different test because of the sensitivity of the spectra to nitric acid concentration, which was not held constant from one test to another.

2.2 Flowsheet Demonstrations

Two experiments were completed to demonstrate the feasibility of dissolving Pu metal at 95 °C. The experiments were performed with and without the addition of B to the dissolving solution. The experimental methods used to carry out the experiments are summarized in the following sections.

2.2.1 *Test Conditions*

The test conditions for the Pu metal dissolutions were selected so that rate measurements at 95 °C could be compared to data reported by Rudisill et al. [3] at higher temperatures. Both experiments were designed to dissolve 3.5 to 4 g of Pu metal in a 10 M HNO_3 solution containing 0.1 M KF targeting a final Pu concentration of 6.75 g/L. The B concentration in the initial experiment was limited to 1 g/L which is consistent with the concentration used in the previous work. Iron, Cr, and Ni were also added to the dissolving solutions at concentrations representative of the concentrations which were measured in the solution from the second batch of Pu metal dissolved for the AFS-2 program in the 6.1D dissolver. The target concentrations in the dissolving solutions for the two experiments are summarized in Table 2-3.

Table 2-3. Target Concentration in Pu Metal Dissolving Solutions

Component	Experiment M1	Experiment M2
HNO_3 (M)	10	10
KF (M)	0.1	0.1
B (g/L)	1	0
Fe (g/L)	3.4 – 3.5	3.4 – 3.5
Cr (g/L)	0.6 – 0.7	0.6 – 0.7
Ni (g/L)	0.3 – 0.4	0.3 – 0.4

2.2.2 *Dissolving Solution Analysis*

Although the intent was to perform the Pu metal dissolutions using 10 M HNO_3, free and total acid analyses of the solutions before and after the dissolutions indicated that the initial acid concentrations were approximately 6 M. The acid analyses are provided in Appendix A. It appears that the total volume of concentrated HNO_3 specified in the work instructions was not used during the preparation of the solutions. The other components of the dissolving solutions were prepared at the correct concentrations. The concentrations of K, B, Fe, Cr, and Ni were confirmed by inductively-coupled plasma emission spectroscopy (ICPES). The ICPES analysis for both solutions is provided in Appendix A. Comparisons of the free acid and ICPES analyses with the concentrations targeted during the solution preparation are provided in Table 2-4. The effects of using a lower acid concentration than intended during the dissolutions are discussed in section 3.1.3.

Table 2-4. Analysis of Pu Metal Dissolving Solutions

Component	Experiment M1		Experiment M2	
	Target	Measured(1)	Target	Measured(1)
HNO_3 (M)	10	6.0	10	6.0
K (KF) (M)	0.1	0.094	0.1	0.101
B (g/L)	1.000	0.981	0	0.055
Fe (g/L)	3.456	3.450	3.456	3.590
Cr (g/L)	0.606	0.594	0.606	0.628
Ni (g/L)	0.373	0.365	0.373	0.406

(1) ± 10% relative standard deviation

2.2.3 *Preparation of Pu Metal*

The metal used in the flowsheet demonstration experiments was cut from coupons of δ-phase Pu received from the FB-Line vault in March 1999; the origin of the metal is unknown. Pictures of the initial coupons are shown in Figure 2-2.

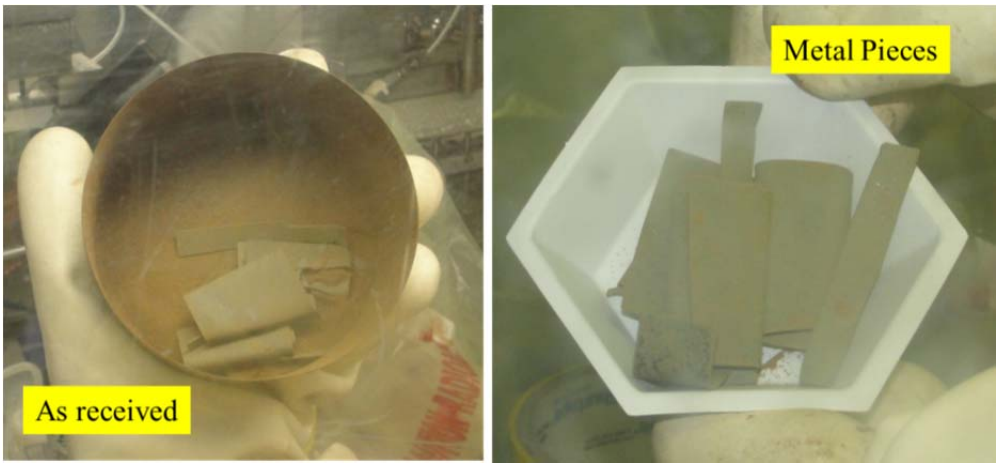

Figure 2-2. Pu Metal Coupons – Source Material for Test Samples

To prepare metal for the demonstration experiments, coupons were cut into pieces with masses which ranged between 3.5 and 4.0 g. A mass in this range was selected to generate approximately 6.75 g/L Pu when dissolved in 500–600 mL of solution. The mass and dimensions of the metal pieces used in the demonstration experiments are provided in Table 2-5. The dimensions of the metal pieces were measured using a micrometer. The calculated density of the metal pieces was approximately 10 g/cm^3. This measurement is lower than expected based on theoretical density which is likely due to the error in the calculated area which is based on measurement of the dimensions of the irregular pieces.

Table 2-5. Mass and Dimensions of Pu Metal Used in Flowsheet Demonstration Experiments

Experiment	Mass (g)	Length (mm)	Width (mm)	Thickness (mm)
M1	3.7826	34.63	11.62	0.93
M2	3.9524	27.50	14.62	0.92

2.2.4 *Pu Metal Dissolving System*

The vessel for the Pu metal dissolutions was fabricated from borosilicate glass by the SRNL Glass Shop. A photograph of the equipment is shown in Figure 2-3. The dissolving vessel was fabricated from a 500-mL, round-bottom flask. Penetrations were added for a condenser, sample port, thermocouple, and N_2 purge (which was not used) with the bottom slightly flattened to facilitate heating and agitation using a hot plate/stirrer (with magnetic stir bar). The temperature was controlled using an external thermocouple monitored by the hot plate. The offgas from the dissolution exited through the water-cooled condenser. Water was recirculated from a beaker to the condenser using a small pump.

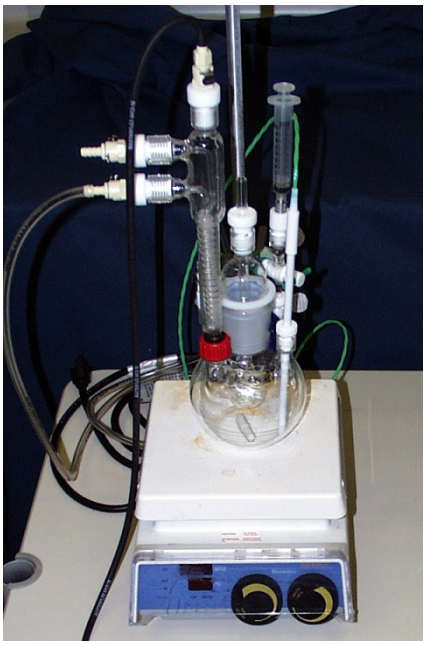

Figure 2-3. Pu Metal Dissolving System

To perform a dissolution test, the Pu metal was initially placed in a perforated glass basket. The basket was suspended in the dissolver by a glass rod held in place by a compression fitting. The compression fitting allowed adjustment of the basket height. Agitation was started at 900 rpm and the hot plate set point was adjusted to 95 °C. When the temperature was reached, the Pu metal was lowered to fully submerge into the dissolving solution and the time clock for the experiment was started. The hot plate maintained the solution temperature at 95 ± 3 °C. At 0.25-h intervals the Pu metal was removed from the dissolver to measure the mass and surface area (i.e., length, width, and thickness of the coupon). Dissolution rates were calculated as the rate of change of the mass-to-surface area ratio as a function of time.

Prior to returning the Pu metal to the dissolving vessel, a 10-mL, disposable syringe was attached to the sample port (see Figure 2-3) using a Luer lock fitting. The stopcock was opened and an approximate 2-mL aliquot of the solution was removed from the dissolver. A UV-visible spectrum of the solution was initially obtained to estimate the concentration of Pu(VI) as the dissolution proceeded. The presence of Pu(VI) in the dissolving solutions was evaluated using the characteristic Pu(VI) peak at 831 nm in nitrate solutions. The solution was subsequently analyzed for ^{239}Pu and ^{241}Am by gamma pulse height analysis (GPHA). Once the sampling was complete, the Pu metal was returned to the dissolving solution and the time clock for the experiment was restarted.

3.0 Results and Discussion

3.1 Simulated Dissolution Studies

3.1.1 *UV-visible Spectroscopic Characterization*

In a typical simulated dissolution experiment, 2-mL samples were collected periodically during the course of heating of the Pu dissolving simulant solution and monitored by UV-visible

spectroscopy. Absorbance spectra exhibit distinct absorbance peaks corresponding to Pu(VI) which are observed to grow in amplitude over time while peaks corresponding to Pu(IV) decline. Spectral data from the first scoping test (Test 0) (Figure 3-1) are shown as an example and are generally representative of spectral data observations for Tests 0–6 (see Appendix D for UV-vis spectra of Tests 1–6). In previous work [5], we found Fe(III), Cr(III) and Cr(VI) absorb in the 350–700 nm range where Pu(IV) absorbs but do not absorb in the 800–850 nm range where Pu(VI) absorbance peaks are located. Figure 3-1 shows the spectra of the Pu solution (Test 0) prepared with Pu(IV) and Cr(III) as well as a comparison spectra of the solution from Tank 7.4. Peaks characteristic of Pu(VI) in ~8.5 M HNO_3 are observed in the solution spectra at 811 and 829 nm when sampled at 4.9 hours. These peaks continue to increase in size as the solution boiling time increases. A gradual reduction in amplitude of multiple Pu(IV) peaks consistent with the oxidation of Pu(IV) to Pu(VI) is also observed especially at 485, 536, 650, and 744 nm. The spectrum from a Tank 7.4 sample (originally sampled on March 12, 2013) is included for comparison and shows somewhat more Pu(VI) than was observed in the 12.9-hour sample of the simulant. The conditions during the scoping simulated dissolution (Test 0) were somewhat

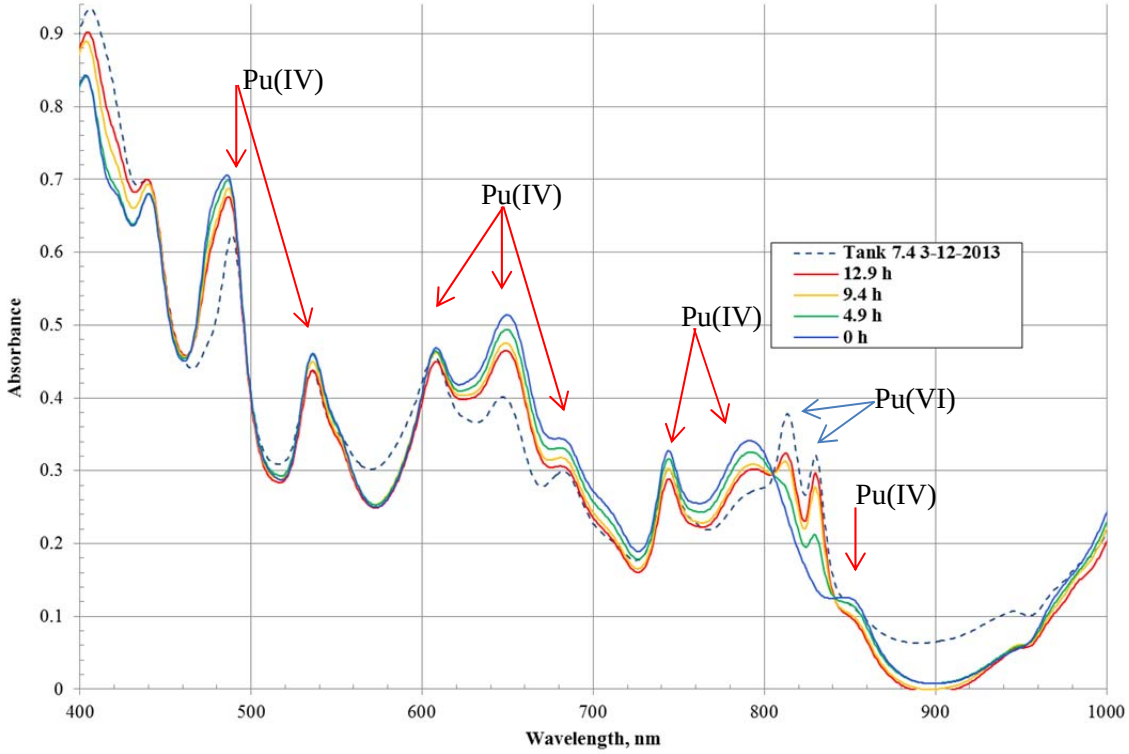

Figure 3-1. Spectra of the simulated Pu dissolving solution showing oxidation of Pu(IV) to Pu(VI) as a function of solution boil time.

different than an actual metal dissolution (nitrogen oxide gasses produced from the metal dissolving process and the corrosion of the vessel would be different), and the time at boil was roughly 1/3 that of the Tank 7.4 solution. The two spectra are, however, very similar when compared.

In Figure 3-1, one can see a modest increase in the absorbance peak at 400–420 nm with heating time. Absorbance in this region is primarily due to Fe(III), Cr(III) and Cr(VI). The small increase in the peak in this region of the spectra could be due to either Cr(VI) accumulation or concentration of the solution due to evaporation.

There are some differences between the Tank 7.4 spectra and the spectra of all of the simulant solutions at 785 nm (see Figure 3-1). The simulant spectra show a peak at 785 nm which becomes smaller with heating time, however, this peak appears to be absent or much smaller in the spectra of the Tank 7.4 sample. This peak likely corresponds to Pu(IV).

The second derivatives of the spectra from Figure 3-1 are included as Figure 3-2 through Figure 3-4. Figure 3-2 shows the range from 400–1000 nm, whereas Figure 3-3 focuses on the changes associated with the ingrowth of Pu(VI) at 811 and 828 nm, and Figure 3-4 focuses on changes between 400 and 500 nm where the peak height of Pu(IV) is decreasing and Cr(VI) may be increasing. Figure 3-3 shows the rate of Pu(VI) ingrowth associated with the peaks at 811 and 829 nm. Figure 3-4 is a plot in the 400–500 nm range where Pu(IV), Fe(III), Cr(III) and Cr(VI) all absorb which confounds interpretation of the spectra. Trends are clearly observed at 404, 414, 421, 441, 466, 474 and 496 nm. Most of these trends are due to Pu(IV) oxidation but changes at 404 nm may be due to Cr(VI) accumulation.

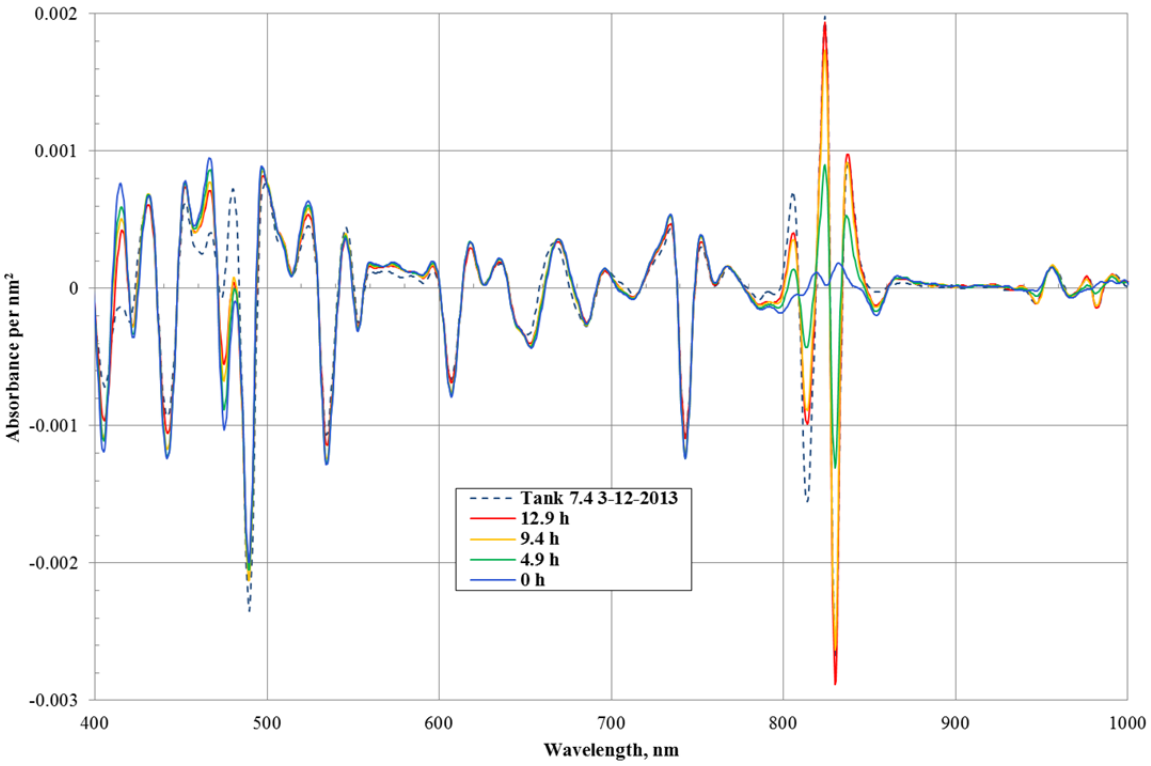

Figure 3-2. Second derivative spectra of the simulated dissolver solution showing oxidation of Pu(IV) to Pu(VI) as a function of solution boil time (800–850 nm) for Test 0.

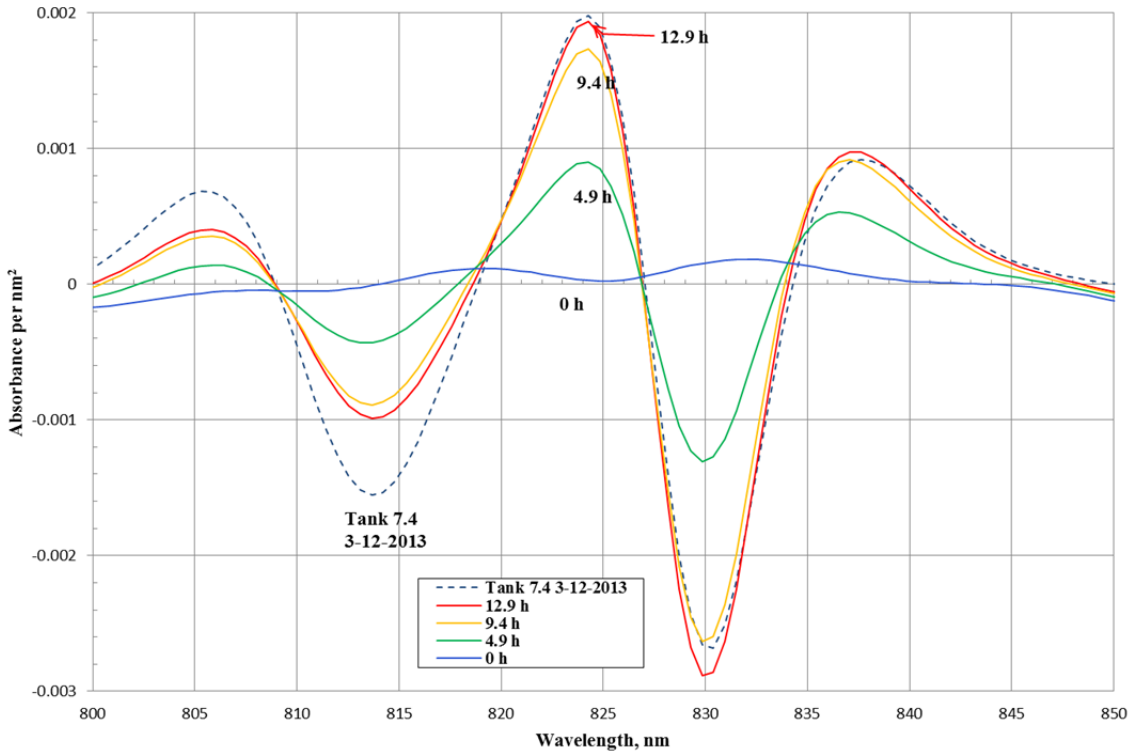

Figure 3-3. Second derivative of the spectra of the simulated dissolver solution showing oxidation of Pu(IV) to Pu(VI) as a function of solution boil time (800–850 nm) for Test 0.

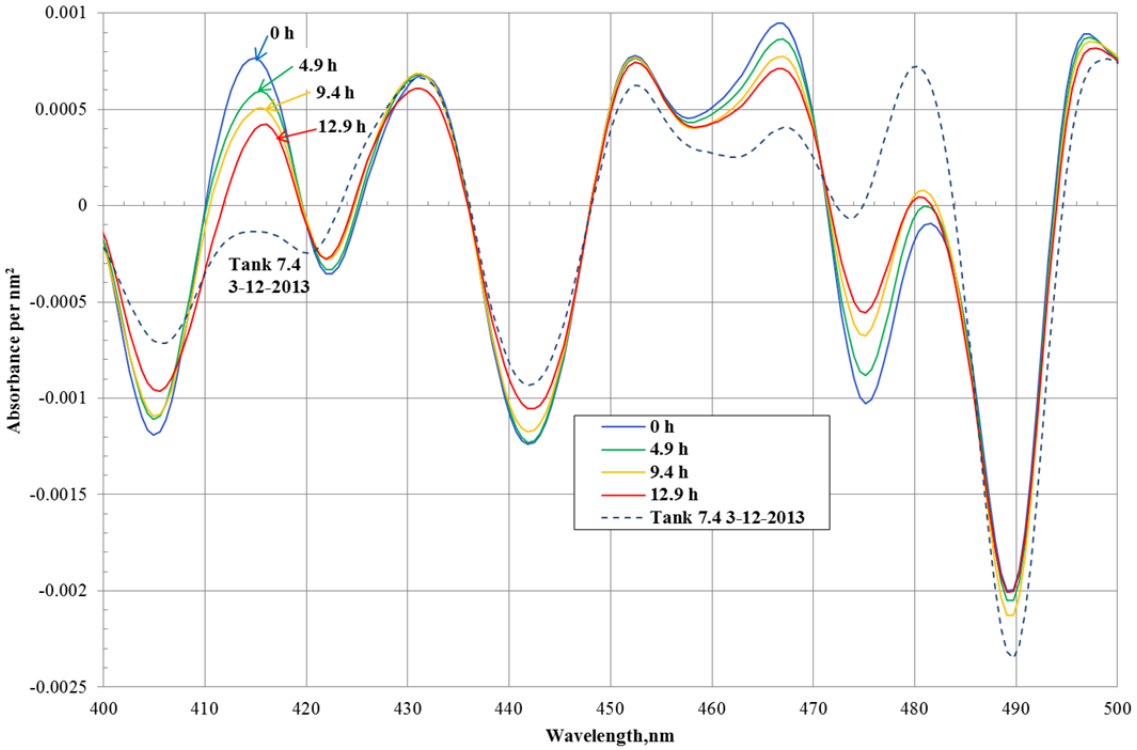

Figure 3-4. Second derivative of the spectra of the simulated dissolver solution showing oxidation of Pu(IV) to Pu(VI) as a function of solution boil time (400–500 nm) for Test 0.

3.1.2 *Effect of HNO_3 Concentration*

Four tests were conducted at or near the respective solution boiling points (Test 0, Test 1, Test 2, and Test 3; Figure 3-5) to determine the effect of HNO_3 concentration on the rate of Pu(VI) ingrowth. These tests (Test 0, Test 1, Test 2, and Test 3) at or near the solution boiling point had very similar rates of Pu(VI) ingrowth (>35% in 50 h). Lower acid molarity (7 M, Test 2 versus 8.1 M, Test 1) would be expected to reduce the oxidation of Cr(III) to Cr(VI) [4] and therefore reduce the ingrowth of Pu(VI). The opposite trend was observed. Pu(VI) was formed at these temperatures (108–116 °C (Test 0–3)) at a higher rate in 7 M HNO_3 (Test 2) than in 8.1 M HNO_3 (Test 1 and 3) or 8.4 M HNO_3 (Test 0). These results (higher oxidation rate in 7 M HNO_3 (Test 2) are consistent with reports by Crocker [1] of increasing the rate of Pu(VI) formation with decreasing HNO_3 concentration for HNO_3 systems without Cr present. Test 3 (8.1 M HNO_3 without Cr in solution) confirms that Cr is not necessary for rapid oxidation of Pu(IV) to Pu(VI) at near boiling temperatures. Data for lower temperature tests (Tests 4–6) are also consistent with lower HNO_3 concentrations having higher Pu(VI) generation rates (at constant temperature), however Test 6 (6 M HNO_3) also has a higher Pu concentration than Tests 0–5 which is also expected to increase the rate of Pu(VI) generation. Additional experimentation would be required to determine the relative effects of Pu and HNO_3 concentration on the increased Pu(IV) oxidation rate which was observed in Test 6.

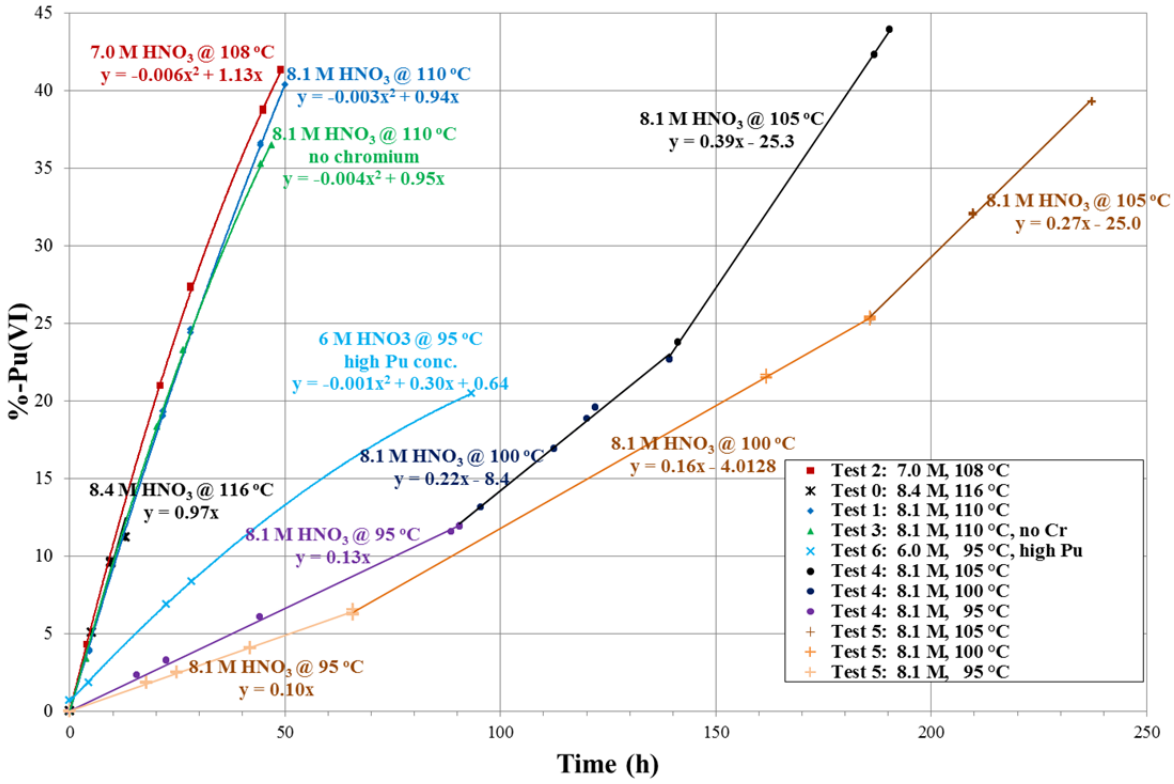

Figure 3-5. Pu(VI) Ingrowth (%) as a Function of Time for Tests 0–6.

3.1.3 *Effect of Temperature*

Lowering the temperature from near boiling to 95 °C was found to decrease the rate of Pu(VI) ingrowth dramatically. For example, at the same HNO_3 concentration (8.1 M) and Pu concentration (3.51 g/L) 5% Pu(VI) was present after 50 hours at 95 °C (Test 5) versus 40% Pu(VI) after 50 hours near boiling (110 °C) (Test 1). Test 4 and Test 5 demonstrate that the rate

of Pu(VI) formation increases with temperature (95 °C<100 °C<105 °C) at constant HNO_3 molarity.

3.1.4 *Effect of Pu Concentration*

Although it was not the specific intent of this study to address the effect of the concentration of individual or total Pu species on the rate of Pu(IV) to Pu(VI) conversion, a number of observations can be made with regard to the simulated dissolution test results. Although there are many sources of error (temperature measurement, volume/weight measurement, and other analytical errors) which contribute to differences between two similar sets of test data, it is nevertheless noteworthy that Test 4 (8.1 M HNO_3) had a higher initial concentration of Pu (3.78 g/L) than Test 5 (8.1 M HNO_3, 3.51 g/L Pu). The higher Pu concentration in Test 4 appears to correspond to higher rates for conversion of Pu(IV) to Pu(VI) at each temperature tested (95 °C, 100 °C, and 105 °C) when compared to Test 5. Test 6 (6 M HNO_3, 95 °C, 6.75 g/L Pu) also had a higher rate for conversion of Pu(IV) to Pu(VI) than Test 4 (8.1 M HNO_3, 95 °C, 3.78 g/L Pu) or Test 5 (8.1 M HNO_3, 95 °C, 3.51 g/L Pu) although it is not possible from this study to determine the relative contribution to this effect of the lower HNO_3 concentration versus the increase in Pu concentration.

3.1.5 *Additional Characterization*

Additional characterization of the simulated Pu dissolution solutions includes the analysis of the initial solution by ICP-ES, total and free acid analyses of the initial and final solutions, and Pu by GPHA for all samples. ICP-ES, total and free acid, and GPHA for reagent and radiochemical solution analyses are included in Appendix A and Appendix B, respectively.

3.2 Flowsheet Demonstrations

3.2.1 *General Observations*

Prior to starting the dissolution experiment, the Pu metal coupon was placed in the glass basket. The solution was then heated to 95 °C and the coupon lowered into the dissolving solution. Almost immediately after the metal was lowered into the solution, brown NO_2 gas filled the dissolver. During each dissolution experiment, the glass basket was removed from the solution at 0.25-h intervals to measure the mass and physical dimensions of the metal to allow the calculation of the dissolution rate (see section 3.2.1). Before the metal was returned to the dissolving vessel, a 2-mL to 3-mL sample of the solution was removed to measure the Pu(VI) concentration by UV-visible spectroscopy (see Figure 3-6 and Figure 3-7) and the ^{239}Pu concentration by GPHA. By UV-visible spectroscopy, no distinguishable differences were observed when comparing the spectral features between the two experiments. These spectra are typical for Pu(IV) in 6 M HNO_3 as described by Marsh et al. [11], notably the peak at ~473 nm and the region between 575 nm and 725 nm as well as the feature around 850 nm. Once the liquid sample was removed, the Pu metal was returned to the dissolving vessel. This procedure was repeated until no Pu metal remained in the glass basket which occurred 1.5 h after starting both experiments. Heating of the dissolving solution continued for an additional 0.25 h to ensure that any small metal fragments which had escaped from the basket had completely dissolved. After the samples at 1.75 h were removed from the vessel, the experiments were terminated. No residues were observed in the solutions after cooling.

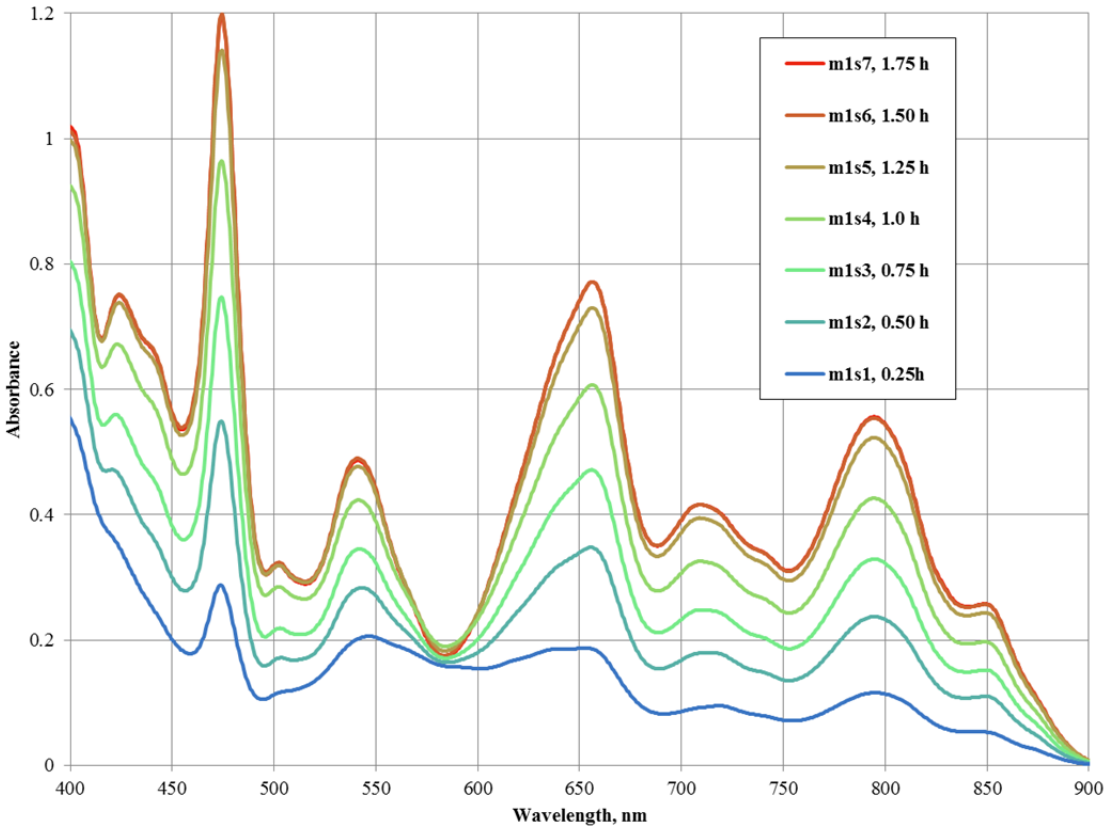

Figure 3-6. Spectra of Pu(IV) Ingrowth During Experiment M1.

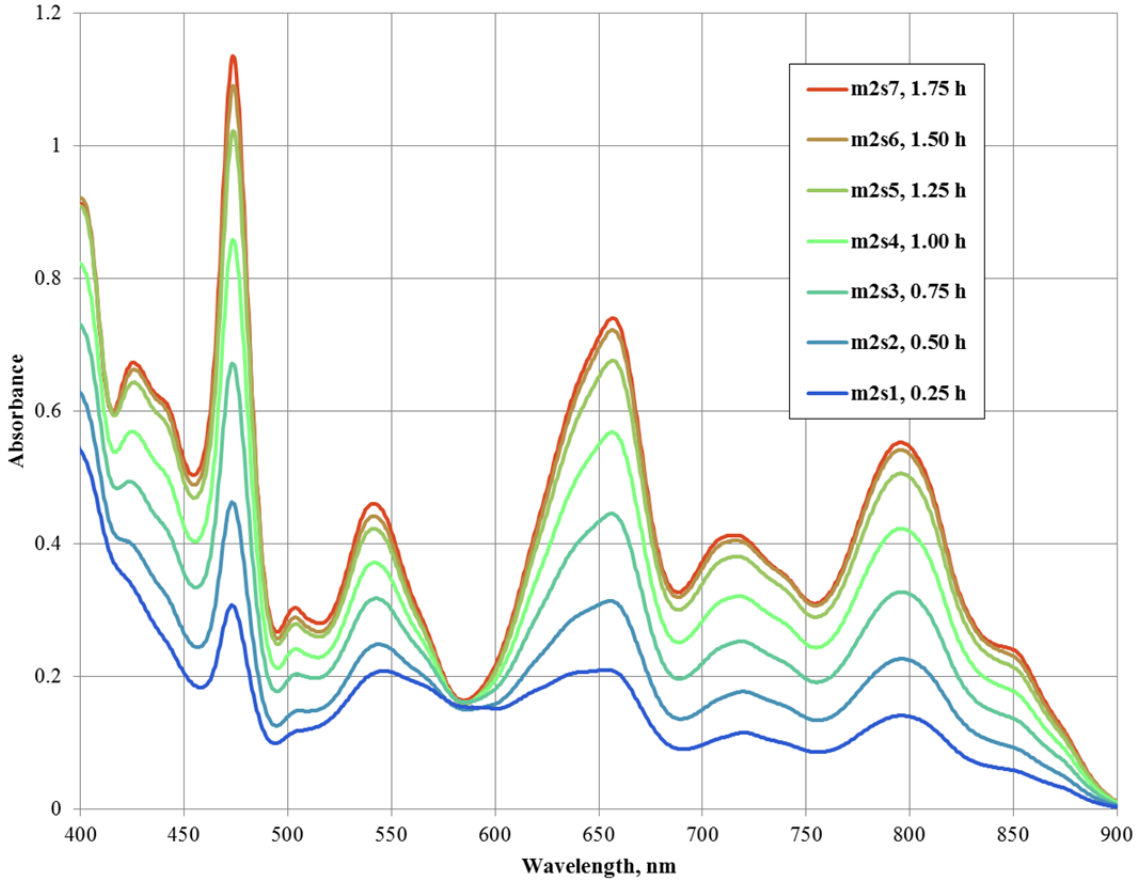

Figure 3-7. Spectra of Pu(IV) Ingrowth During Experiment M2.

3.2.2 *Sample Analysis*

The GPHA for the samples generated during the Pu metal dissolutions are provided in Appendix B. Activities for both ^{239}Pu and ^{241}Am were measured. The ^{239}Pu activities were converted to total Pu values by assuming the metal coupons were weapons grade Pu containing 94 wt % ^{239}Pu. Before the concentrations were correlated with the dissolution time, they were corrected for the small change in volume which occurred due to the removal of samples and evaporation losses; although, a small concentrating effect would be expected in the 6.1D dissolver due to evaporation. The volumes of solution at the conclusion of Experiments M1 and M2 decreased by 32 and 26 mL, respectively. A small correction was also made for the amount of material removed in samples prior to completing the experiment. The mass of Pu removed in each 2-mL to 3-mL sample ranged between 2 and 22 mg. The magnitude of the corrections ranged from <1% to 4%. The procedure used to correct the concentrations and the calculated values are provided in Appendix B.

The corrected Pu and Am concentrations as functions of the dissolution time are plotted in Figure 3-8 and Figure 3-9 for Experiments M1 and M2, respectively. The error bars in the figures reflect the one sigma uncertainty in the GPHA (Table B-13 and Table B-14). The uncertainties associated with the volume measurements used to calculate the corrected actinide concentrations were found to be insignificant compared to the uncertainties in the radiochemical analyses.

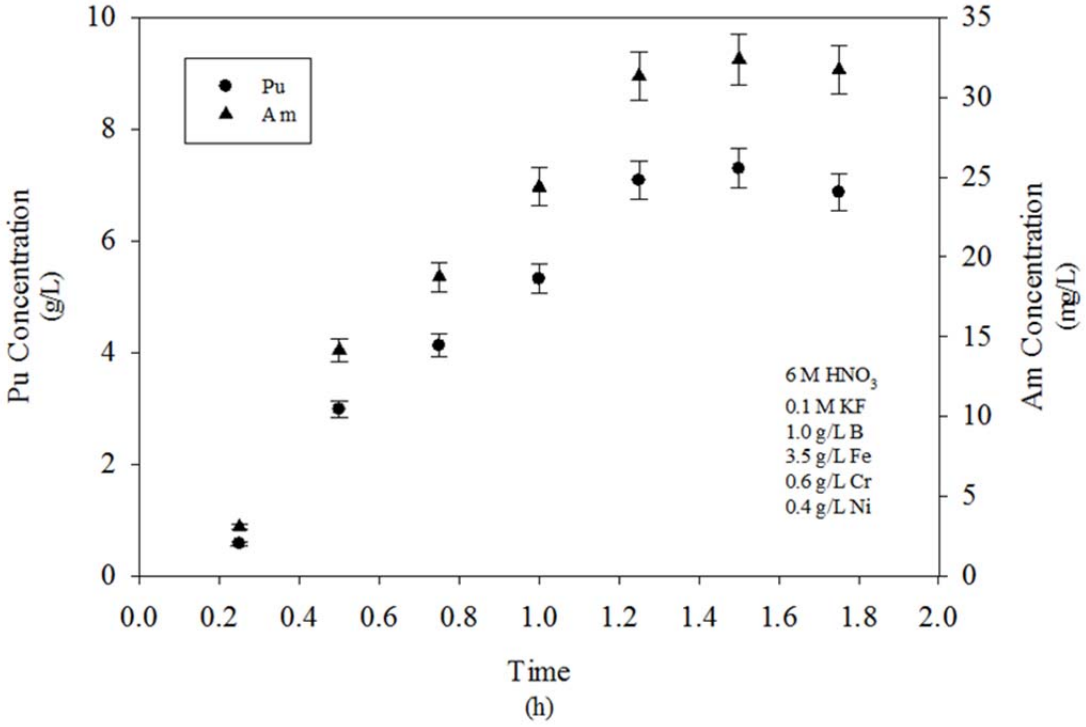

Figure 3-8. Corrected Actinide Concentrations in Experiment M1

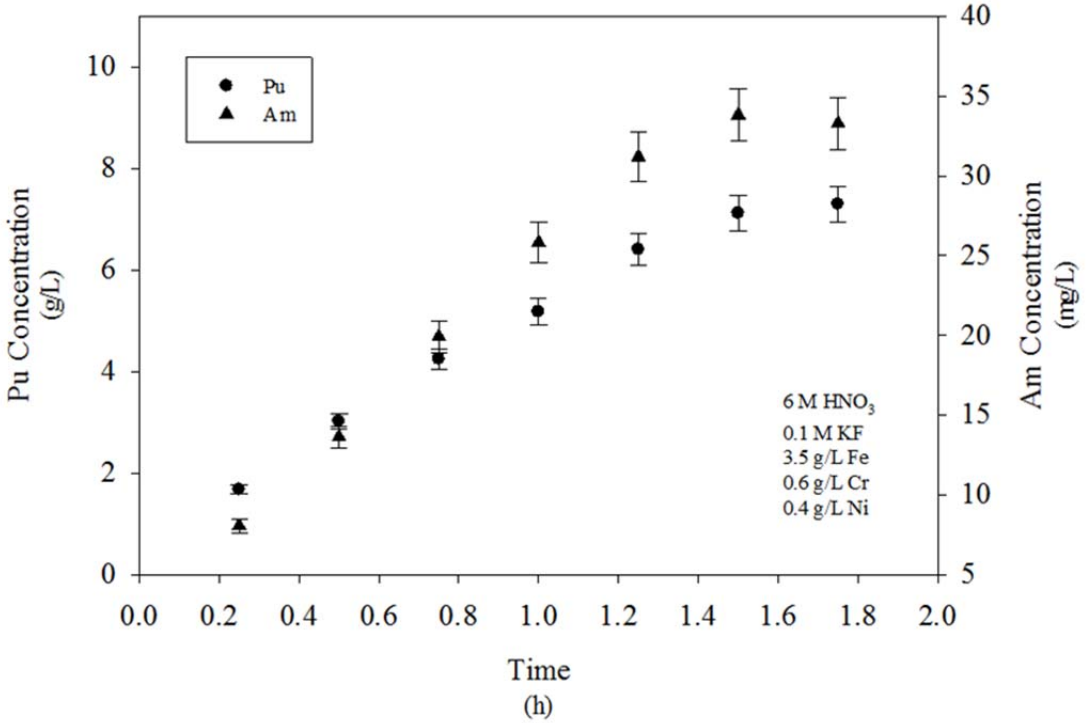

Figure 3-9. Corrected Actinide Concentrations in Experiment M2

The Pu and Am concentrations (Figure 3-8 and Figure 3-9) are consistent with the observation that complete dissolution was accomplished in each experiment. Each figure showed a steady increase in the actinide concentration with time which approached a constant value at the end of the experiment. Table 3-1 provides a comparison of the maximum corrected concentration (at the end of an experiment) to the concentration calculated from the mass of Pu metal and the volume of the dissolving solution used in the experiment. The uncertainties in the Pu concentrations calculated from the metal masses and initial volumes of solution were based on a 1% relative standard deviation in each of the measurements. The calculations are summarized in Appendix B.

Table 3-1. Comparison of Pu Concentrations Based on Corrected Value and Metal Mass

Experiment	(Corrected) Pu Concentration (g/L)	(Mass-based) Pu Concentration (g/L)	Difference (%)
M1	7.05 ± 0.35	6.74 ± 0.10	4.56
M2	7.11 ± 0.36	6.74 ± 0.10	5.42

The Pu concentrations for each experiment show reasonably good agreement. In each case, the corrected concentration appears biased high. This is likely due to uncertainties in the radiochemical analyses and inaccuracies in the estimated volume losses during the experiments.

To calculate the amount of Pu and Am metal dissolved as a function of time, the estimated solution volume and the Pu and Am concentrations at each sample time were used to calculate the mass of Pu and Am in solution. The calculated mass was expressed as a percentage of the total mass dissolved based on the maximum mass of Pu and Am in solution at the end of the experiment. The calculations are summarized in Appendix B. Figure 3-10 and Figure 3-11 show the mass of Pu and Am dissolved as a function of time for experiments M1 and M2, respectively. The error bars in the figures were calculated using the one sigma uncertainties in the GPHA (Table B-13 and Table B-14) and propagation of error techniques. The uncertainties associated with the volume measurements used to calculate the amounts of the metals dissolved were found to be insignificant compared to the uncertainties in the radiochemical analyses. The error analysis is summarized in Appendix B.

The percentages of Pu and Am dissolved during each experiment were very close in magnitude which indicates that the metals dissolved uniformly. The curves for each experiment were used to approximate the time required for complete dissolution of the metal coupons. The values are given in Table 3-2.

Table 3-2. Time Required for Complete Dissolution of Pu Metal Coupons

Experiment	Dissolution Time (h)
M1	1.5
M2	1.75

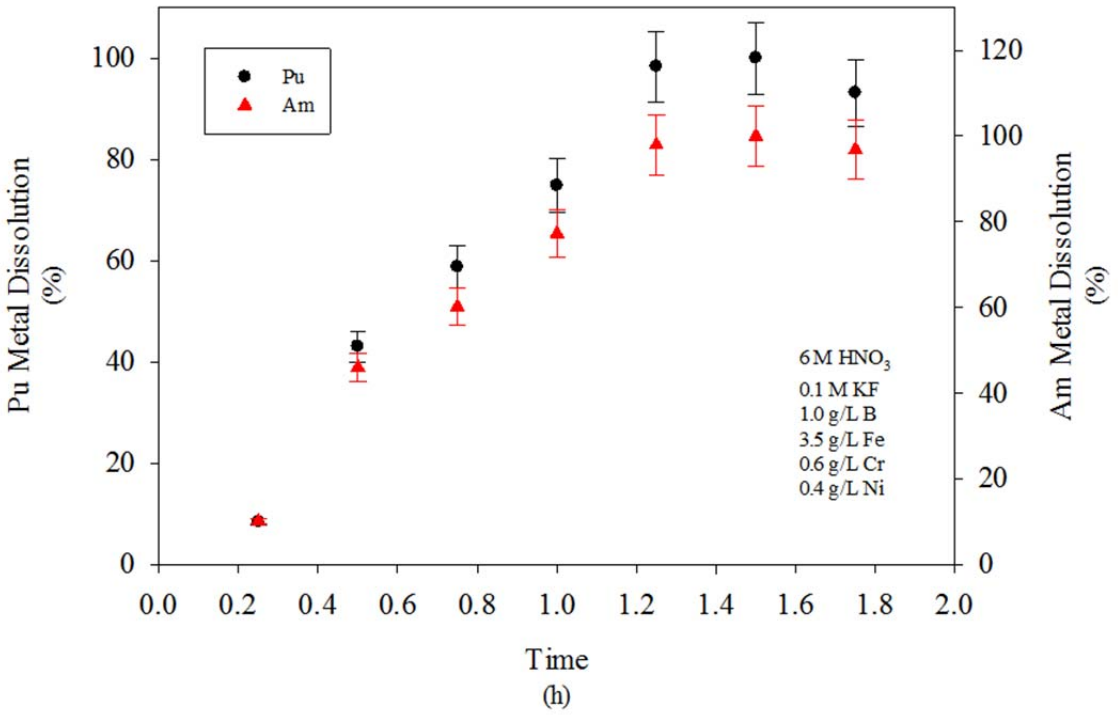

Figure 3-10. Actinide Metal Dissolution in Experiment M1

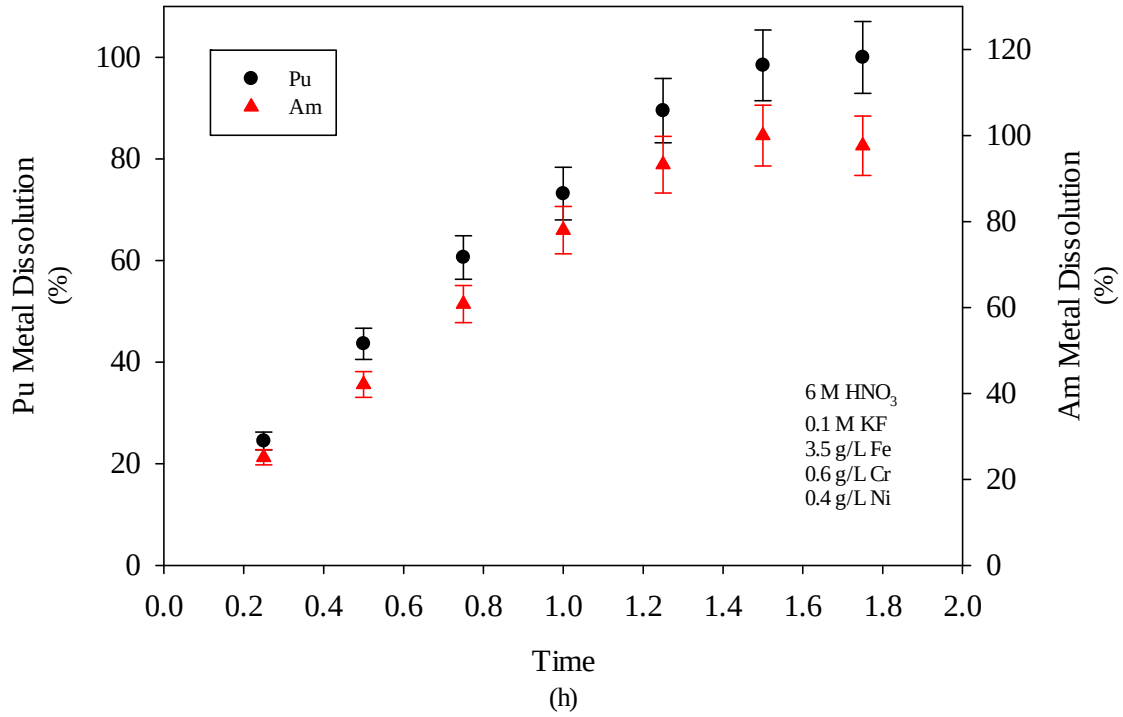

Figure 3-11. Actinide Metal Dissolution in Experiment M2

3.2.3 *Dissolution Rate Measurements*

The Pu metal was removed from the dissolving vessel at 0.25-hr intervals to measure the mass and physical dimensions (i.e., length, width, and thickness) of the coupons. Dissolution rates were calculated as the rate of change of the mass-to-surface area ratio as a function of time. The measurements were repeated until the coupons no longer retained a rectangular geometry (1.25 h into the dissolution for both experiments). The dissolution rate data for the experiments are provided in Appendix C. To calculate the dissolution rate, the mass-to-surface area ratios for the Pu metal coupons are plotted as a function of the time on Figure 3-12 and Figure 3-13. Linear regressions were performed for each data set. The slope of the line through the data is the dissolution rate and the uncertainty of the dissolution rate is the standard deviation of the slope of the line in units of mg/cm^2-min.

The addition of 1 g/L B to the solution had a small effect on the Pu dissolution rate, reducing the value from 5.5 to 5.1 $mg/min\text{-}cm^2$. This observation is consistent with the trend in data reported by Rudisill et al. [3]. Figure 3-14 shows rate data for dissolutions performed by Rudisill et al. [3] using 10 M HNO_3 at constant KF concentrations and temperature for 1 and 2 g/L B. Increasing the B concentration from 1 to 2 g/L had a much smaller effect on the dissolution rate than the small increase in fluoride concentration. The dissolutions were carried out in borosilicate glass vessels which under these reaction conditions corrode. The corrosion accounts for the small amount of B in the analysis of the M2 solution to which B was not directly added.

Due to an error in the preparation of the dissolving solutions, the starting HNO_3 concentrations used for the two Pu metal dissolutions in this work were nominally 6 M, rather than the 10 M target value. However, both experiments demonstrated that Pu metal could be dissolved (at 95 °C) up to a concentration of 6.75 g/L using this concentration of acid without the generation of PuO_2 solids. We do not expect the Pu metal dissolution rate at higher HNO_3 concentrations (i.e., 8 to 10 M) to be greatly different. This conclusion is based on previous work by Rudisill et al. [3] in which triplicate Pu metal dissolution rate measurements were made in 8 and 10 M HNO_3 solutions containing 0.1 M KF and 1 g/L B at 100 °C (Figure 3-15). The data show that the dissolution rate was not a strong function of the HNO_3 concentration. The dissolution rate decreased slightly when the HNO_3 concentration increased from 8 to 10 M. Miner et al. [12] also observed a decrease in Pu metal dissolution rates above approximately 3 M HNO_3 during experiments performed at 1–5 M HNO_3, 0.01–0.13 M HF, and 23–69 °C. The decrease in the Pu metal dissolution rate as the HNO_3 concentration increases (above 3 M) was attributed to the passivation of the metal surface by the highly oxidizing solutions [12].

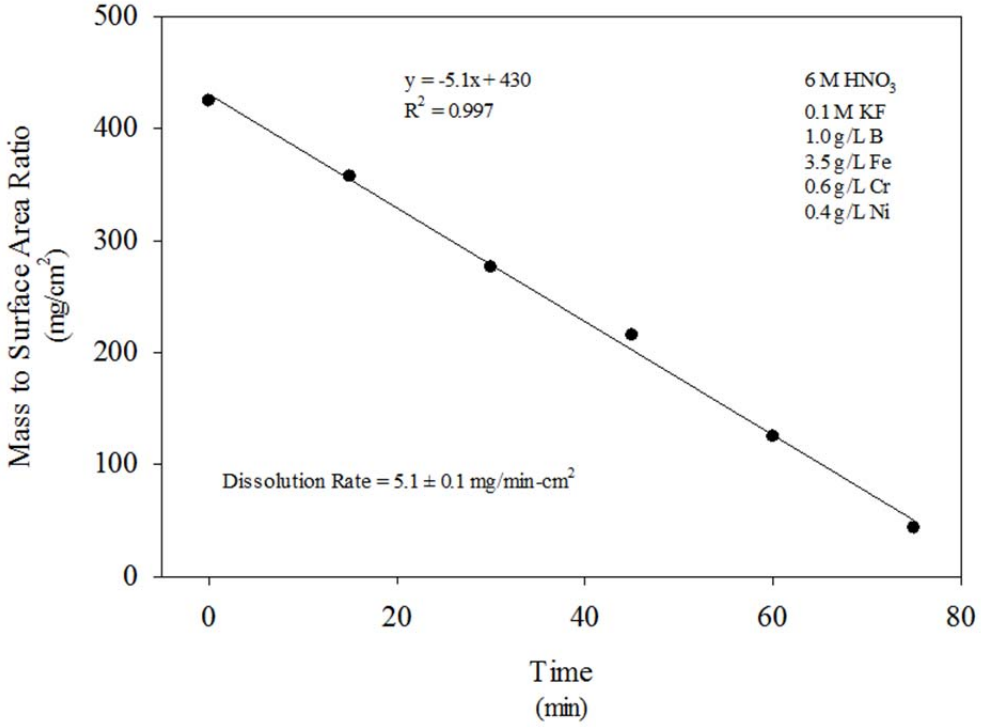

Figure 3-12. Dissolution Rate Calculation for Experiment M1

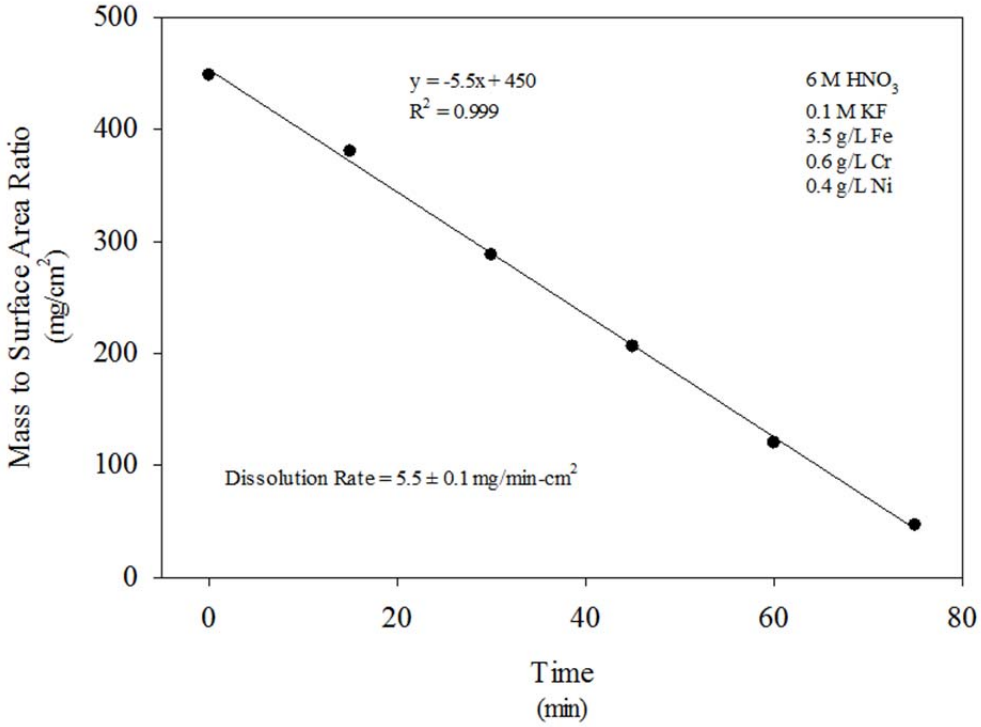

Figure 3-13. Dissolution Rate Calculation for Experiment M2

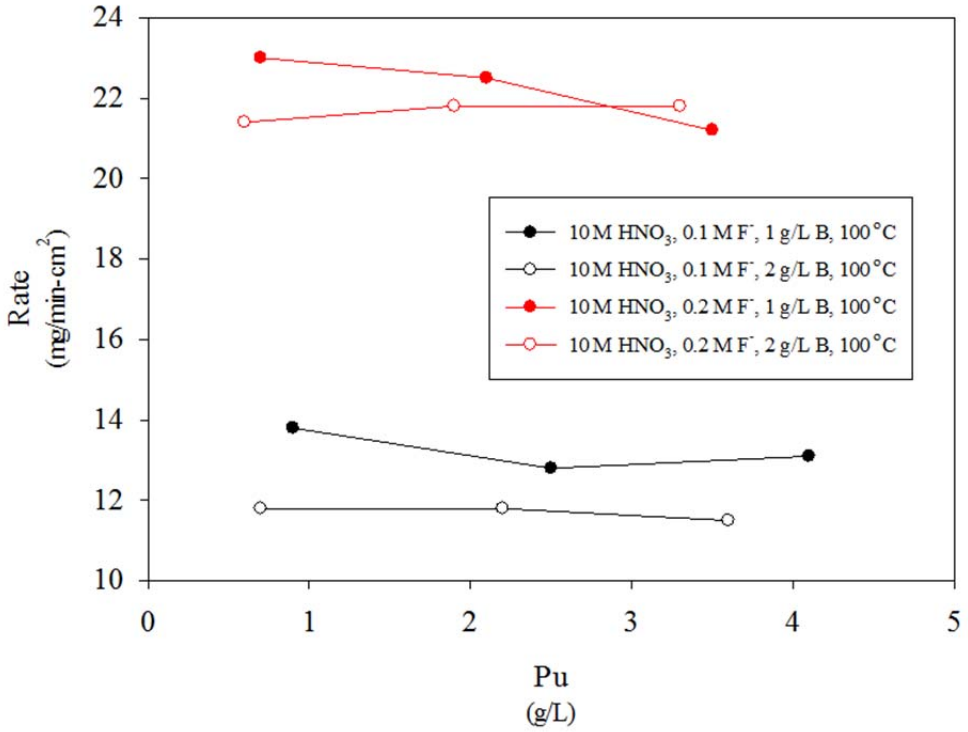

Figure 3-14. Effect of B Concentration on Pu Metal Dissolution Rate [3]

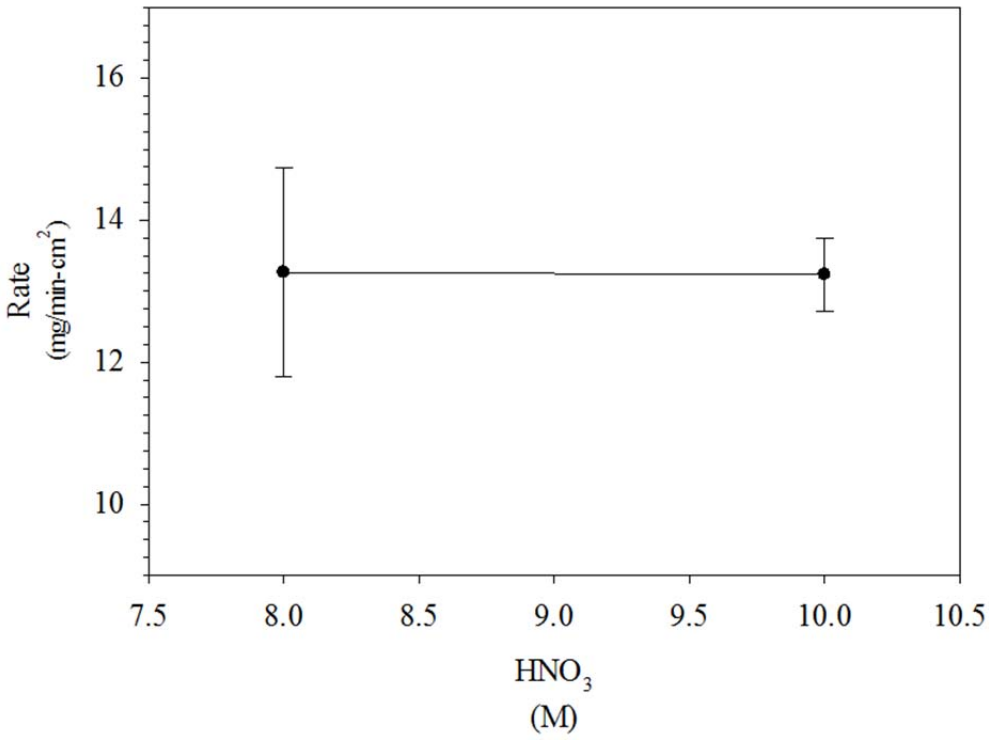

Figure 3-15. Effect of HNO_3 Concentration on Pu Metal Dissolution Rate [3]

3.2.4 *Scale-up to H-Canyon Dissolvers*

It is difficult to correlate the time required to completely dissolve a batch of Pu metal in an H-Canyon dissolver based on laboratory dissolutions due to differences in the surface-to-volume ratios of the metals dissolved. However, Holcomb [2] prepared a correlation which relates the dissolution rate to the time required to completely dissolve a Pu metal button. The correlation (Figure 3-16) is a plot of dissolution rate versus the time required to dissolve one typical SRS alpha-phase button. Although the data in Figure 3-16 is for alpha-phase metal, the relationship between the dissolution rate and the time required for complete dissolution would hold for delta-phase metal of approximately the same mass and geometry [2].

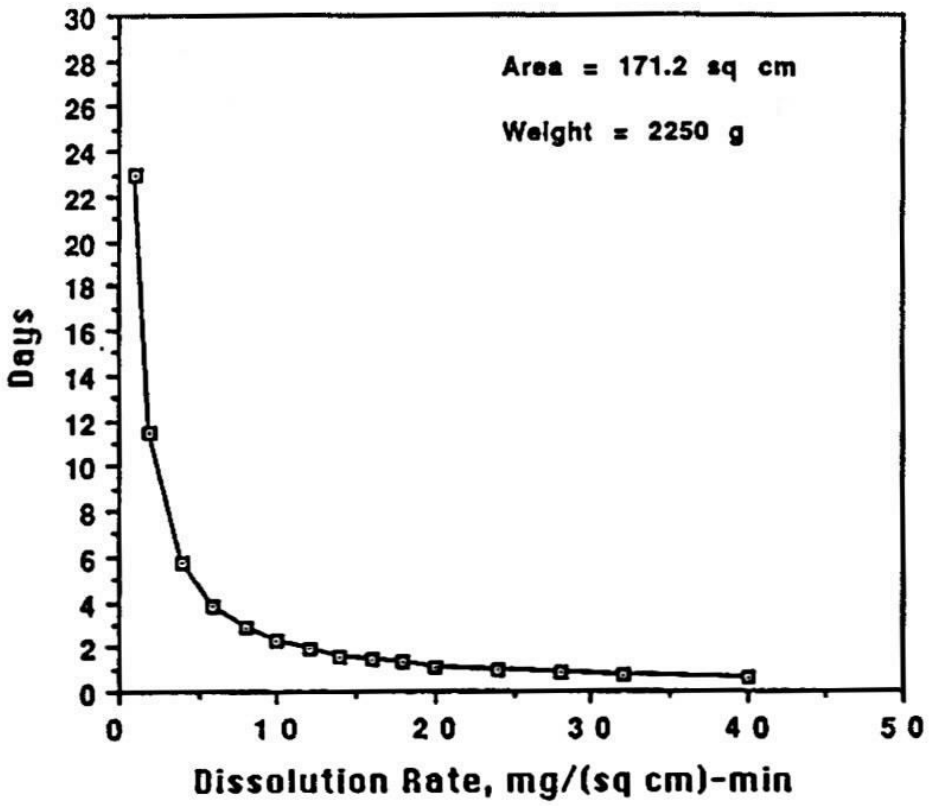

Figure 3-16. Estimated Time for the Dissolution of a Pu Metal Button [2]

To use Figure 3-16 to predict the time required to dissolve a Pu button at a specified rate, one must assume that each individual button in a charge will dissolve at the same rate as a single button. This is a reasonable assumption given that the final Pu concentration is low (i.e., <6.75 g/L). For a dissolution rate of approximately 5 mg/min-cm^2 (similar to the rate measured in the Pu metal dissolution experiments at 95 °C), the estimated time required to completely dissolve a button is nearly 5 days (120 h).

A second method to estimate the time required to completely dissolve a batch of Pu metal in an H-Canyon dissolver is to scale the actual dissolution times from the dissolver using the results from this study and data reported by Rudisill et al. [3]. In the previous study, Rudisill et al. measured a Pu dissolution rate of 11.3 ± 1.9 mg/min-cm^2 using a 10 M HNO_3 solution containing 0.1 M KF and 1 g/L B at boiling (112–116 °C). In this study, the Pu dissolution rate for a 6 M HNO_3 solution containing 0.1 M KF and 1 g/L B at 95 °C was 5.1 ± 0.1 mg/min-cm^2. Assuming the difference in the HNO_3 and transition metal (e.g., Fe, Cr, and Ni) concentrations in the

solutions do not significantly affect the rate of dissolution, decreasing the temperature from boiling to 95 °C reduced the rate by approximately a factor of two. The dissolution time for the second and third batches of Pu metal dissolved in the 6.1D dissolver were 36 and 54 h. The dissolutions were performed using a 9–10 M HNO_3 solution containing 0.1 M KF and approximately 1.5 g/L B at boiling. Therefore, based on the two laboratory studies, the dissolution time for a dissolving solution of similar composition at 95 °C would likely range between 72 and 108 h depending on the surface area of the Pu buttons. This range is reasonably consistent with the estimated time to completely dissolve a Pu button based on the correlation developed by Holcomb [2].

4.0 Conclusions

In simulated Pu dissolutions studies, lowering the temperature from near boiling to 95 °C had the effect of reducing the oxidation rate of Pu(IV) to Pu(VI). At near boiling conditions, the rate of conversion of Pu(IV) to Pu(VI) was not affected significantly by the Cr concentration or by changing the molarity of HNO_3 in the range of 7 M to 8.5 M (>35% Pu(VI) in 50 h). Conversion of Pu(IV) to Pu(VI) without Cr present as a catalyst is consistent with literature reports of HNO_3 oxidation of Pu(IV) to Pu(VI) at 98 °C in HNO_3 alone [1]. In the same literature report [1], the rate of conversion to Pu(VI) decreases as HNO_3 molarity increases in the range 7 M to 8.5 M HNO_3 (at 98 °C). At 95 °C we observed a higher rate of conversion of Pu(IV) to Pu(VI) (>5% Pu(VI) at 95°C in 50 h for 8.1 M HNO_3) than rates reported in the literature [1] at a higher temperature (98 °C; <5% Pu(VI) in 50 h for 7–8 M HNO_3), however, these literature studies are at lower Pu concentrations and without Cr, Fe, or Ni in solution.

Two small-scale experiments were performed to demonstrate the dissolution of Pu metal up to 6.75 g/L in concentrated HNO_3 solutions with KF at 95 °C. The use of 6 M HNO_3 containing 0.1 M KF with and without the presence of B resulted in complete dissolution of the metal in 1.5 to 1.75 h. In these experiments, Fe, Cr, and Ni were added at concentrations representative of the values in the solution generated from the dissolution of the second batch of Pu metal in H-Canyon. Plutonium metal dissolution rates measured during the experiments ranged from 5.1 mg/min-cm^2 (with B) to 5.5 mg/min-cm^2 (without B). The presence of 1 g/L B in the solution only had a small effect on the Pu metal dissolution rate. Due to an error in the preparation of the dissolving solutions, the starting HNO_3 used for the dissolutions was nominally 6 M rather than the 10 M target value. We do not expect the change in the Pu metal dissolution rate at higher HNO_3 concentrations (i.e., 8–10 M) to be greatly different. This conclusion is based on previous work by Rudisill et al. [3] which showed that the dissolution rate was not a strong function of the HNO_3 concentration.

A correlation developed by Holcomb [2] for the time required to dissolve a Pu metal button was used to estimate the time required to dissolve a batch of Pu metal in an H-Canyon dissolver using 6–10 M HNO_3 containing 0.05–0.2 M KF at 95 °C. For a dissolution rate of approximately 5 mg/min-cm^2, the estimated time required to completely dissolve a button is nearly 5 days (120 h). The Pu metal dissolution time for the same flowsheet was also estimated based on the Batch 2 and 3 dissolution times in the 6.1D dissolver and Pu metal dissolution rates measured in this study and by Rudisill et al. [3]. Data from the present and previous studies show that the Pu metal dissolution rate decreases by a factor of approximately two when the temperature decreased from boiling (112 to 116 °C) to 95 °C. Therefore, the time required to dissolve a batch of Pu metal in an H-Canyon dissolver at 95 °C would likely double (from 36 to 54 h) and require 72 to 108 h depending on the surface area of the Pu metal

5.0 Recommendations

A Pu metal dissolution flowsheet utilizing 6–10 M HNO_3 containing 0.05–0.2 M KF (with 0–2 g/L B) at 95 °C is recommended to reduce the oxidation of Pu(IV) to Pu(VI). However, the time required to completely dissolve a batch of Pu metal will increase by approximately a factor of two as compared to previous H-canyon experience with Batches 2 and 3 (assuming the KF concentration is maintained at nominally 0.1 M) [5]. Although hydrogen generation was not measured in these studies, previously reported studies by Rudisill et al. [3] are applicable to the flowsheet modifications related to hydrogen generation under bounding, higher-temperature conditions.

6.0 Future Work

Additional studies could be beneficial to determine the independent effects of Pu, Cr, and HNO_3 concentration at a lower temperature (95 °C) where these effects are likely to have a more pronounced effect than at boiling. Based on the literature [1], increasing HNO_3 molarity at 95 °C should further decrease the rate of Pu(VI) ingrowth, and this effect is likely to have a greater effect at lower temperature than near boiling. Additional studies at 95 °C to better define conditions for further reduction of the rate of Pu(VI) ingrowth could be carried out using the same approach as the studies reported herein to confirm the effect of increasing the molarity of HNO_3 on the rate of Pu(VI) ingrowth for concentrations greater than 8.5 M HNO_3. Additionally, literature studies [1] indicate that increasing the Pu concentration would be expected to increase the rate of Pu(VI) ingrowth. The contribution of total Pu concentration and Cr concentration on the rate of Pu(VI) ingrowth at 95 °C were not directly addressed in these studies but could be defined using a similar experimental approach.

7.0 References

1. I. H. Crocker, *Oxidation of Pu (IV) to Pu (VI) in Solutions of Nitric Acid, Aluminum Nitrate, Sodium Nitrate, and Uranyl Nitrate,* CRDC 697AECL No. 48. Atomic Energy of Canada Limited, Chalk River Project, 1957.
2. H. P. Holcomb, *Laboratory-scale Dissolution of Delta-phase Plutonium Metal*, WSRC-TR-90-0101, Westinghouse Savannah River Company, Aiken, SC (March 1990).
3. T. S. Rudisill and R. A. Pierce, *Dissolution of Plutonium Metal in 8–10 M Nitric Acid*, SRNL–STI-2012-00043, Rev. 1, Savannah River National Laboratory, Aiken, SC, July 2012.
4. E. A. Kyser to W. H. Clifton, *Preliminary Investigation of the Pu Valence State in Pu Tanks 12.2 and 7.4*, SRNL-L3100-2013, 000046, Savannah River National Laboratory, Aiken, SC, March 26, 2013.
5. E. A. Kyser to W. H. Clifton, *Preliminary Investigation: Reduction of Cr(VI) to Cr(III) in Anion Exchange Feedstock for AFS-2*, SRNL-L3100-2013-00048, Savannah River National Laboratory, Aiken, SC, March 28, 2013.
6. W. H. Smith, G. Purdy, *Chromium in Aqueous Nitrate Process Streams: Corrosion of 316 Stainless Steel and Chromium Speciation*, LA-UR-94-2400, Los Alamos National Laboratory, Los Alamos, NM, 1994.
7. T. W. Newton and M. J. Burkhart, *The Preparation and Properties of a Chromium(III)-Plutonium(V) Complex*, Inorg Chem, Vol. 10, No. 10, 1971, 2323–7.
8. M. V. Posvol'skii and I. I. Tsirlin, *Induced Reactions in Radiochemistry I. Induced Oxidation by Bichromate*, Sov Radiochem, Vol. 10, No. 5, 530–3, 1968.
9. M. V. Posvol'skii and I. I. Tsirlin, *Induced Reactions in Radiochemistry II. Catalysis of the Induced Oxidation of Plutonium by Chromium(VI)*, Sov Radiochem, Vol. 12, No. 2, 327–31, 1970.
10. E.A. Kyser, P. E. O'Rourke, *Sample Results from the Treatment of Tank 12.2 with FS for Pu(VI) Reduction*, SRNL-L3100-2013-00127, Rev. 0, Savannah River National Laboratory, Aiken SC, July 24, 2013.
11. S. F. Marsh, R. S. Day, D. K. Veirs, *Spectrophotometric Investigation of the Pu(IV) Nitrate Complex Sorbed by Ion Exchange Resins*, LA-12070, Los Alamos National Laboratory, Los Alamos, NM (June 1991).
12. F. J. Miner, J. H. Nairn, and J. W. Berry, *Dissolution of Plutonium in Dilute Nitric Acid*, I&EC Product Research and Development, **8**, pp. 402–405 (1969).

Appendix A. Reagent Analysis

Simulated Pu Dissolutions – Acid Analyses

Table A-1. Free and Total Acid Concentration for Simulated Pu Dissolving Solutions

Experiment	Sample ID	Description	Free Acid(1) (M)	Total Acid(1) (M)
Test 1	T1S1b	Before heating	6.45	8.04
Test 1	T1S6b	After heating	6.38	8.16
Test 2	T2S7	Before heating	5.40	7.00
Test 2	T2S13b	After heating	5.48	7.06
Test 3	T3S14b	Before heating	NA	8.00
Test 3	T3S20b	After heating	7.28	8.14
Test 4	T4S25b	Before heating	7.00	7.94
Test 4	T4S30b	After heating	7.10	8.00
Test 4	T4S33b	After heating	6.96	8.01
Test 5	T5S35b	Before heating	7.14	8.38
Test 5	T5S41b	After heating	8.05	8.51
Test 5	T5S43b	After heating	8.14	8.61
Test 6	T6S1b	Before heating	5.92	6.33
Test 6	T6S6b	After heating	6.00	6.39

(1) ± 10% relative standard deviation
NA = not analyzed

Simulated Pu Dissolutions – ICPES Analyses

Samples of the solution prior to heating were analyzed for metals by ICPES. The analysis for each solution is given in Table A-2, Table A-3, and Table A-4

Table A-2. ICPES Analysis for Simulated Pu Dissolving Solutions

Element	Test 1		Test 2	
	Concentration (mg/L)	Uncertainty (% RSD)	Concentration (mg/L)	Uncertainty (% RSD)
Ag	<1.06	N/A	<1.06	N/A
Al	6.81	10.1	12.2	10.1
B	1640	10	1570	10
Ba	<0.53	N/A	<0.53	N/A
Be	<0.1	N/A	<0.1	N/A
Ca	4.07	10	7.8	10
Cd	<1.22	N/A	<1.22	N/A
Ce	<0.577	N/A	<0.577	N/A
Co	<0.211	N/A	<0.211	N/A
Cr	625	10	618	10
Cu	<2.75	N/A	<2.75	N/A
Fe	3640	10	3610	10
Gd	<2.35	N/A	<2.35	N/A
K	3740	10.1	3560	10
La	<0.78	N/A	<0.78	N/A
Li	0.211	12.3	0.253	15.6
Mg	0.1	10	0.51	10
Mn	<0.91	N/A	<0.91	N/A
Mo	<0.83	N/A	<0.83	N/A
Na	34.1	10	57.6	10
Ni	401	10	396	10
P	<18.2	N/A	<18.2	N/A
Pb	<0.98	N/A	<0.98	N/A
S	<80	N/A	<80	N/A
Sb	<2.9	N/A	<2.9	N/A
Si	20	10.1	25.4	10.1
Sn	<1.16	N/A	<1.16	N/A
Sr	<0.1	N/A	<0.1	N/A
Th	<18.6	N/A	<18.6	N/A
Ti	<0.35	N/A	<0.35	N/A
U	<44	N/A	<44	N/A
V	<0.55	N/A	<0.55	N/A
Zn	<1.98	N/A	<1.98	N/A
Zr	<0.88	N/A	<0.88	N/A

Table A-3. ICPES Analysis for Simulated Pu Dissolving Solutions (continued)

Element	Test 3		Test 4	
	Concentration (mg/L)	Uncertainty (% RSD)	Concentration (mg/L)	Uncertainty (% RSD)
Ag	<1.06	N/A	<1.06	N/A
Al	13.5	10	16.7	10.2
B	1610	10	1590	10
Ba	<0.53	N/A	<0.53	N/A
Be	<0.1	N/A	<0.1	N/A
Ca	5.97	10	15.8	10
Cd	<1.22	N/A	<1.22	N/A
Ce	<1.15	N/A	<1.15	N/A
Co	<0.422	N/A	<0.422	N/A
Cr	3.75	13.9	612	10
Cu	<2.75	N/A	<2.75	N/A
Fe	3620	10	3590	10
Gd	<2.35	N/A	<2.35	N/A
K	3680	10	3660	10
La	<0.78	N/A	<0.78	N/A
Li	0.282	12.8	0.324	11.9
Mg	0.7	10	0.77	10
Mn	<0.91	N/A	<0.91	N/A
Mo	<1.66	N/A	<1.66	N/A
Na	65.5	10	79.8	10
Ni	383	10	403	10.1
P	<18.2	N/A	<18.2	N/A
Pb	<1.96	N/A	<1.96	N/A
S	<160	N/A	<160	N/A
Sb	<5.79	N/A	<5.79	N/A
Si	19.3	10.1	21.4	10.1
Sn	<2.32	N/A	<2.32	N/A
Sr	<0.1	N/A	<0.1	N/A
Th	<18.6	N/A	<18.6	N/A
Ti	<0.35	N/A	<0.35	N/A
U	<44	N/A	<44	N/A
V	<0.55	N/A	<0.55	N/A
Zn	<1.98	N/A	<1.98	N/A
Zr	<0.88	N/A	<0.88	N/A

Table A-4. ICPES Analysis for Simulated Pu Dissolving Solutions (continued)

Element	Test 5		Test 6	
	Concentration (mg/L)	Uncertainty (% RSD)	Concentration (mg/L)	Uncertainty (% RSD)
Ag	<5.3	N/A	<5.3	N/A
Al	<38.7	N/A	<38.7	N/A
B	1450	10.1	1050	10.1
Ba	<3.5	N/A	<3.5	N/A
Be	<0.5	N/A	<0.5	N/A
Ca	13.6	11.4	<8.45	N/A
Cd	<7	N/A	<7	N/A
Ce	<56.6	N/A	<56.6	N/A
Co	<10.6	N/A	<10.6	N/A
Cr	584	10	644	10
Cu	<9.1	N/A	21.2	21.2
Fe	3380	10	3650	10
Gd	<9.6	N/A	<9.6	N/A
K	3550	10.3	3800	10.3
La	<7.1	N/A	<7.1	N/A
Li	<31.8	N/A	<31.8	N/A
Mg	<48.2	N/A	<48.2	N/A
Mn	<4.55	N/A	<4.55	N/A
Mo	<74.7	N/A	<74.7	N/A
Na	<218	N/A	<218	N/A
Ni	409	10.6	443	10.2
P	1220	10.2	2740	10.5
Pb	<736	N/A	<736	N/A
S	<7500	N/A	<7500	N/A
Sb	<145	N/A	<145	N/A
Si	<96.7	N/A	<96.7	N/A
Sn	<100	10.1	<100	N/A
Sr	<74.6	N/A	<74.6	N/A
Th	<59.6	N/A	<100	N/A
Ti	<21	N/A	<21	N/A
U	<487	N/A	<487	N/A
V	<3.55	N/A	<3.55	N/A
Zn	<9.9	N/A	<9.9	N/A
Zr	<110	N/A	<110	N/A

Pu Metal Dissolution – Acid Analyses

Samples of the solutions prepared for Experiments M1 and M2 before and after the Pu metal dissolutions were analyzed for free and total acid by titration. Multiple samples were analyzed to determine the actual starting concentrations of HNO_3. The data for these analyses are provided in Table A-5.

Table A-5. Free and Total Acid Concentration for Pu Metal Dissolving Solutions

Experiment	Sample ID	Description	Free Acid(1) (M)	Total Acid(1) (M)
M1	M1S0b	Before dissolution	5.73	6.13
M1	M1S0b dup	Before dissolution	6.24	6.21
M1	M1S8	After dissolution	5.79	6.27
M1	M1S9 dup	After dissolution	5.92	6.34
M2	M2S0b	Before dissolution	5.77	6.20
M2	M2S0b dup	Before dissolution	6.24	6.25
M2	M2S8	After dissolution	5.81	6.25
M2	M2S9 dup	After dissolution	5.82	6.33

(1) ± 10% relative standard deviation

The free and total acid concentrations for the dissolving solutions are reasonably consistent. The average free acid concentration in each solution prior to the dissolution is 6.0 M. Even though 1 g/L B (as H_3BO_3) was added to dissolving solution for Experiment M1, the HNO_3 concentration is still approximately 6.0 M since the addition of the H_3BO_3 added <0.05 M to the free acid total.

Pu Metal Dissolution – ICPES Analysis

Samples of the solution prior to the dissolution of the Pu metal were analyzed for metals by ICPES. The analysis for each solution is given in Table A-6.

Table A-6. ICPES Analysis for Pu Metal Dissolving Solutions

Element	Experiment M1		Experiment M2	
	Concentration (mg/L)	Uncertainty (% RSD)	Concentration (mg/L)	Uncertainty (% RSD)
Ag	<0.78	NA	<0.78	NA
Al	<23.6	NA	60.4	10.0
B	981	10	55	11.2
Ba	<5.58	NA	<5.58	NA
Ca	3.7	25.1	7.04	11.4
Cd	<5.62	NA	<5.62	NA
Ce	<16.3	NA	<16.3	NA
Co	<12.8	NA	<12.8	NA
Cr	594	10	628	10.0
Cu	5.64	11.1	5.85	11.8
Fe	3450	10.7	3590	11.1
K	3660	10	3950	10.0
La	<1.59	NA	<1.59	NA
Li	<32.6	NA	<32.6	NA
Mg	<7.14	NA	<7.14	NA
Mn	<0.9	NA	<0.9	NA
Mo	<12.2	NA	<12.2	NA
Na	<246	NA	<246	NA
Nb	<15.7	NA	<15.7	NA
Nd	<22.5	NA	<22.5	NA
Ni	365	10.1	406	10.1
P	<66.3	NA	<66.3	NA
Pb	<78.9	NA	<78.9	NA
Re	<78.2	NA	<78.2	NA
S	<17.3	NA	<17.3	NA
Si	43.6	10.7	449	10
Sn	<8.7	NA	<8.7	NA
Sr	<23	NA	<23	NA
Ti	<2.37	NA	<2.37	NA
V	<27.5	NA	<27.5	NA
Zn	<9.7	NA	<9.7	NA
Zr	<210	NA	<210	NA

Appendix B. Radiochemical Solution Analysis

GPHA Data for Simulated Pu Dissolutions

Table B-1. GPHA for Simulated Pu Dissolution Experiment Test 1

Sample ID	Time (h)	^{239}Pu Activity (dpm/mL)	1 sigma Uncertainty (%)	^{241}Am Activity (dpm/mL)	1 sigma Uncertainty (%)
T1S1	0	5.41E+08	5.00	1.90E+06	5.00
T1S2	4.67	5.41E+08	5.00	1.92E+06	5.00
T1S3	21.67	5.28E+08	5.00	1.84E+06	5.00
T1S4	28.08	4.92E+08	5.00	1.97E+06	5.00
T1S5	44.33	4.88E+08	5.00	1.88E+06	5.00
T1S6	50.08	5.13E+08	5.00	1.93E+06	5.00

Table B-2. GPHA for Simulated Pu Dissolution Experiment Test 2.

Sample ID	Time (h)	^{239}Pu Activity (dpm/mL)	1 sigma Uncertainty (%)	^{241}Am Activity (dpm/mL)	1 sigma Uncertainty (%)
T2S8	0	5.18E+08	5.00	2.10E+06	5.00
T2S9	4.00	5.00E+08	5.00	2.01E+06	5.00
T2S10	21.00	5.29E+08	5.00	2.04E+06	5.00
T2S11	28.17	5.30E+08	5.00	2.16E+06	5.00
T2S12	45.00	5.24E+08	5.00	1.96E+06	5.00
T2S13	49.00	5.49E+08	5.00	2.12E+06	5.00

Table B-3. GPHA for Simulated Pu Dissolution Experiment Test 3

Sample ID	Time (h)	^{239}Pu Activity (dpm/mL)	1 sigma Uncertainty (%)	^{241}Am Activity (dpm/mL)	1 sigma Uncertainty (%)
T3S14	0	5.15E+08	5.00	1.91E+06	5.00
T3S15	3.83	6.00E+08	5.00	1.94E+06	5.00
T3S16	20.33	5.52E+08	5.00	1.92E+06	5.00
T3S17	26.37	5.49E+08	5.00	1.93E+06	5.00
T3S18	44.33	5.20E+08	5.00	1.93E+06	5.00
T3S19	46.83	5.21E+08	5.0	1.96E+06	5.00

Table B-4. GPHA for Simulated Pu Dissolution Experiment Test 4.

Sample ID	Time (h)	^{239}Pu Activity (dpm/mL)	1 sigma Uncertainty (%)	^{241}Am Activity (dpm/mL)	1 sigma Uncertainty (%)
T4S25	0	5.63E+08	5.00	1.92E+06	5.00
T4S26	15.58	5.51E+08	5.00	1.95E+06	5.00
T4S27	22.50	5.46E+08	5.00	1.98E+06	5.00
T4S28	44.09	5.83E+08	5.00	2.16E+06	5.00
T4S29	88.50	6.02E+08	5.00	2.15E+06	5.00
T4S30	90.50	5.47E+08	5.00	2.29E+06	5.00
T4S31	95.50	5.31E+08	5.00	2.23E+06	5.00
T4S32	112.50	6.10E+08	5.00	2.01E+06	5.00
T4S33	120.00	5.84E+08	5.00	1.97E+06	5.00

Table B-5. GPHA for Simulated Pu Dissolution Experiment Test 5

Sample ID	Time (h)	^{239}Pu Activity (dpm/mL)	1 sigma Uncertainty (%)	^{241}Am Activity (dpm/mL)	1 sigma Uncertainty (%)
T5S35a	0	5.02E+08	5.00	1.93E+06	5.00
T5S36	17.75	5.52E+08	5.00	2.02E+06	5.00
T5S37	24.75	4.98E+08	5.00	2.06E+06	5.00
T5S38	41.75	5.58E+08	5.00	1.94E+06	5.00
T5S39	65.75	5.31E+08	5.00	2.02E+06	5.00
T5S40	161.75	5.26E+08	5.00	2.05E+06	5.00
T5S41	185.75	5.12E+08	5.00	1.96E+06	5.00
T5S42	209.75	5.25E+08	5.00	2.02E+06	5.00
T5S43a	237.25	5.30E+08	5.00	2.04E+06	5.00

Table B-6. GPHA for Simulated Pu Dissolution Experiment Test 6.

Sample ID	Time (h)	^{239}Pu Activity (dpm/mL)	1 sigma Uncertainty (%)	^{241}Am Activity (dpm/mL)	1 sigma Uncertainty (%)
T6S1a	0	9.09E+08	5.00	2.46E+08	5.00
T6S2	4.33	9.73E+08	5.00	2.52E+08	5.00
T6S3	22.33	8.83E+08	5.00	2.39E+08	5.00
T6S4	28.33	9.51E+08	5.00	2.45E+08	5.00
T6S5	93.33	9.12E+08	5.00	2.41E+08	5.00

The Pu and Am activities given in Table B-1 through Table B-6 were converted to a mass basis using the specific activities of ^{239}Pu and ^{241}Am (1.38E+11 and 7.63E+12 dpm/g, respectively) which were calculated from the isotope half-life. The total Pu concentrations were subsequently calculated by assuming the ^{239}Pu content of weapons grade Pu is 94 wt %. The Pu and Am concentrations for the samples from each dissolution experiment are provided in Table B-7 through Table B-12

Table B-7. Actinide Concentrations in Samples from Simulated Pu Dissolution Experiment Test 1

Sample ID	Time (h)	Pu Concentration (g/L)	1 sigma Uncertainty (%)	Am Concentration (mg/L)	1 sigma Uncertainty (%)
T1S1	0	4.17	5.00	0.249	5.00
T1S2	4.67	4.17	5.00	0.252	5.00
T1S3	21.67	4.07	5.00	0.241	5.00
T1S4	28.08	3.79	5.00	0.258	5.00
T1S5	44.33	3.76	5.00	0.246	5.00
T1S6	50.08	3.95	5.00	0.253	5.00

Table B-8. Actinide Concentrations in Samples from Simulated Pu Dissolution Experiment Test 2

Sample ID	Time (h)	Pu Concentration (g/L)	1 sigma Uncertainty (%)	Am Concentration (mg/L)	1 sigma Uncertainty (%)
T2S8	0	3.99	5.00	0.275	5.00
T2S9	4.00	3.85	5.00	0.263	5.00
T2S10	21.00	4.08	5.00	0.267	5.00
T2S11	28.17	4.09	5.00	0.283	5.00
T2S12	45.00	4.04	5.00	0.257	5.00
T2S13	49.00	4.23	5.00	0.278	5.00

Table B-9. Actinide Concentrations in Samples from Simulated Pu Dissolution Experiment Test 3

Sample ID	Time (h)	Pu Concentration (g/L)	1 sigma Uncertainty (%)	Am Concentration (mg/L)	1 sigma Uncertainty (%)
T3S14	0	3.97	5.00	0.250	5.00
T3S15	3.83	4.63	5.00	0.254	5.00
T3S16	20.33	4.26	5.00	0.252	5.00
T3S17	26.37	4.23	5.00	0.253	5.00
T3S18	44.33	4.01	5.00	0.253	5.00
T3S19	46.83	4.02	5.00	0.257	5.00

Table B-10. Actinide Concentrations in Samples from Simulated Pu Dissolution Experiment Test 4

Sample ID	Time (h)	Pu Concentration (g/L)	1 sigma Uncertainty (%)	Am Concentration (mg/L)	1 sigma Uncertainty (%)
T4S25	0	4.34	5.00	0.252	5.00
T4S26	15.58	4.25	5.00	0.256	5.00
T4S27	22.50	4.21	5.00	0.260	5.00
T4S28	44.09	4.49	5.00	0.283	5.00
T4S29	88.50	4.64	5.00	0.282	5.00
T4S30	90.50	4.22	5.00	0.300	5.00
T4S31	95.50	4.09	5.00	0.292	5.00
T4S32	112.50	4.70	5.00	0.263	5.00
T4S33	120.00	4.50	5.00	0.258	5.00

Table B-11. Actinide Concentrations in Samples from Simulated Pu Dissolution Experiment Test 5

Sample ID	Time (h)	Pu Concentration (g/L)	1 sigma Uncertainty (%)	Am Concentration (mg/L)	1 sigma Uncertainty (%)
T5S35a	0	3.87	5.00	0.253	5.00
T5S36	17.75	4.26	5.00	0.265	5.00
T5S37	24.75	3.84	5.00	0.270	5.00
T5S38	41.75	4.30	5.00	0.254	5.00
T5S39	65.75	4.09	5.00	0.265	5.00
T5S40	161.75	4.05	5.00	0.269	5.00
T5S41	185.75	3.95	5.00	0.257	5.00
T5S42	209.75	4.05	5.00	0.265	5.00
T5S43a	237.25	4.09	5.00	0.267	5.00

Table B-12. Actinide Concentrations in Samples from Simulated Pu Dissolution Experiment Test 6

Sample ID	Time (h)	Pu Concentration (g/L)	1 sigma Uncertainty (%)	Am Concentration (mg/L)	1 sigma Uncertainty (%)
T6S1a	0	7.01	5.00	32.2	5.00
T6S2	4.33	7.50	5.00	33.0	5.00
T6S3	22.33	6.81	5.00	31.3	5.00
T6S4	28.33	7.33	5.00	32.1	5.00
T6S5	93.33	7.03	5.00	31.6	5.00

GPHA Data for Pu Dissolutions

The ^{239}Pu and ^{241}Am activities measured by GPHA for the samples of solution from each Pu dissolution experiment are provided in Table B-13 and Table B-14.

Table B-13. GPHA for Pu Dissolution Experiment M1

Sample ID	Dissolution Time (h)	^{239}Pu Activity (dpm/mL)	1 sigma Uncertainty (%)	^{241}Am Activity (dpm/mL)	1 sigma Uncertainty (%)
M1S1	0.25	7.51E+07	5.93	2.35E+07	5.00
M1S2	0.50	3.87E+08	5.00	1.08E+08	5.00
M1S3	0.75	5.35E+08	5.00	1.43E+08	5.00
M1S4	1.00	6.90E+08	5.00	1.86E+08	5.00
M1S5	1.25	9.19E+08	5.00	2.39E+08	5.00
M1S6	1.50	9.46E+08	5.00	2.47E+08	5.00
M1S7	1.75	8.91E+08	5.00	2.42E+08	5.00

Table B-14. GPHA for Pu Dissolution Experiment M2

Sample ID	Dissolution Time (h)	^{239}Pu Activity (dpm/mL)	1 sigma Uncertainty (%)	^{241}Am Activity (dpm/mL)	1 sigma Uncertainty (%)
M2S1	0.25	2.18E+08	5.18	6.15E+07	5.00
M2S2	0.50	3.92E+08	5.00	1.04E+08	5.00
M2S3	0.75	5.51E+08	5.00	1.52E+08	5.00
M2S4	1.00	6.72E+08	5.00	1.97E+08	5.00
M2S5	1.25	8.31E+08	5.00	2.38E+08	5.00
M2S6	1.50	9.24E+08	5.00	2.58E+08	5.00
M2S7	1.75	9.47E+08	5.00	2.54E+08	5.00

The Pu and Am activities given in Table B-13 and Table B-14 were converted to a mass basis using the specific activities of ^{239}Pu and ^{241}Am (1.38E+11 and 7.63E+12 dpm/g, respectively) which were calculated from the isotope half-life. The total Pu concentrations were subsequently calculated by assuming the ^{239}Pu content of weapons grade Pu is 94 wt %. The Pu and Am concentrations for the samples from each dissolution experiment are provided in Table B-15 and Table B-16.

Table B-15. Actinide Concentrations in Samples from Pu Dissolution Experiment M1

Sample ID	Dissolution Time (h)	Pu Concentration (g/L)	1 sigma Uncertainty (%)	Am Concentration (mg/L)	1 sigma Uncertainty (%)
M1S1	0.25	0.579	5.93	3.08	5.00
M1S2	0.50	2.98	5.00	14.2	5.00
M1S3	0.75	4.12	5.00	18.7	5.00
M1S4	1.00	5.32	5.00	24.4	5.00
M1S5	1.25	7.08	5.00	31.3	5.00
M1S6	1.50	7.29	5.00	32.4	5.00
M1S7	1.75	6.87	5.00	31.7	5.00

Table B-16. Actinide Concentrations in Samples from Pu Dissolution Experiment M2

Sample ID	Dissolution Time (h)	Pu Concentration (g/L)	1 sigma Uncertainty (%)	Am Concentration (mg/L)	1 sigma Uncertainty (%)
M2S1	0.25	1.68	5.18	8.06	5.00
M2S2	0.50	3.02	5.00	13.6	5.00
M2S3	0.75	4.25	5.00	19.9	5.00
M2S4	1.00	5.18	5.00	25.8	5.00
M2S5	1.25	6.41	5.00	31.2	5.00
M2S6	1.50	7.12	5.00	33.8	5.00
M2S7	1.75	7.30	5.00	33.3	5.00

Evaporation Rate

The Pu and Am concentrations in each sample were corrected for small changes in volume which occurred due to sample removal and evaporation losses from the dissolver. A small correction was also made for the Pu and Am removed in samples prior to completing the experiment. The volume of the samples removed from the dissolver varied between 2 and 3 mL. A small volume of solution was also spilled when several samples were removed during Experiment M1. The volume of solution removed at each sample time during Experiments M1 and M2 are provided in Table B-17 and Table B-18, respectively.

Table B-17. Sample Volumes for Pu Dissolution Experiment M1

Sample ID	Sample Volume (mL)	Lost Volume (mL)	Total Volume Removed (mL)
M1S1	2.2	1.0	3.2
M1S2	2.1	0.3	2.4
M1S3	2.0	0.0	2.0
M1S4	2.0	0.0	2.0
M1S5	2.1	0.0	2.1
M1S6	2.0	0.0	2.0
M1S7	2.2	1.0	3.2
Other Samples	4.0	0.0	4.0
Total	18.6	2.3	20.9

Table B-18. Sample Volumes for Pu Dissolution Experiment M2

Sample ID	Sample Volume (mL)	Total Volume Removed (mL)
M2S1	2.2	2.2
M2S2	2.4	2.4
M2S3	2.2	2.2
M2S4	2.3	2.3
M2S5	2.6	2.6
M2S6	2.0	2.0
M2S7	2.3	2.3
Totals	16.0	16.0

The evaporation rate was estimated from the initial and final dissolving solution volumes and the total volume removed during sampling. The calculations are summarized in Table B-19.

Table B-19. Evaporation Rate during Pu Dissolution Experiments

Experiment No.	Initial Volume (mL)	Final Volume (mL)	Volume Removed (mL)	Evaporated Volume (mL)	Dissolution Time (h)	Evaporation Rate (mL/h)
M1	561	525	20.9	15.1	1.75	8.6
M2	586	560	16.0	10.0	1.75	5.7

The calculations in Table B-19 assume the evaporation rate was constant during the dissolving experiments. The estimated volumes of solution in the dissolver for each dissolution experiment prior to the removal of the sample are given in Table B-20 and Table B-21.

Table B-20. Estimated Dissolver Volumes for Pu Dissolution Experiment M1

Sample ID	Dissolution Time (h)	Dissolver Volume (mL)
M1S1	0.25	559
M1S2	0.50	553
M1S3	0.75	549
M1S4	1.00	545
M1S5	1.25	541
M1S6	1.50	536
M1S7	1.75	532

Table B-21. Estimated Dissolver Volumes for Pu Dissolution Experiment M2

Sample ID	Dissolution Time (h)	Dissolver Volume (mL)
M2S1	0.25	585
M2S2	0.50	581
M2S3	0.75	577
M2S4	1.00	573
M2S5	1.25	570
M2S6	1.50	566
M2S7	1.75	562

Corrected Actinide Concentrations

The corrected Pu and Am concentrations were calculated by adjusting for the change in volume and accounting for the small amount of material removed from the dissolving solution in each sample. The generalized expression used to calculate the corrected concentrations ($C_{t_{corrected}}$) at sample time t is given as equation B.1,

$$C_{t_{corrected}} = \frac{C_t V_t + \sum_{i=1}^{t-1} C_i V_{s_i}}{V_0} \qquad (B.1)$$

where C_t and C_i are measured concentrations (Table B-15 and Table B-16), V_t is the estimated volume (Table B-20 and Table B-21), Vs_i is the total volume removed during sampling (Table B-17 and Table B-18), and V_0 is the initial volume (Table B-19). The corrected concentrations for the actinides are given in Table B-22 and Table B-23.

Table B-22. Corrected Actinide Concentrations for Pu Dissolution Experiment M1

Sample ID	Dissolution Time (h)	$Pu_{corrected}$ Concentration (g/L)	$Am_{corrected}$ Concentration (mg/L)
M1S1	0.25	0.577	3.07
M1S2	0.50	2.95	14.0
M1S3	0.75	4.05	18.4
M1S4	1.00	5.20	23.8
M1S5	1.25	6.88	30.4
M1S6	1.50	7.05	31.3
M1S7	1.75	6.62	30.6

Table B-23. Corrected Actinide Concentrations for Pu Dissolution Experiment M2

Sample ID	Dissolution Time (h)	$Pu_{corrected}$ Concentration (g/L)	$Am_{corrected}$ Concentration (mg/L)
M2S1	0.25	1.68	8.04
M2S2	0.50	3.00	13.5
M2S3	0.75	4.20	19.7
M2S4	1.00	5.10	25.4
M2S5	1.25	6.28	30.6
M2S6	1.50	6.96	33.0
M2S7	1.75	7.11	32.5

Uncertainty in Actinide Concentrations Based on Metal Mass

The expected concentration of Pu at the end of the dissolution ($C_{Pu_{final}}$) was calculated from the mass of metal (M_{Pu}) and the initial volume (V_0) of solution used in the experiment (Table 3-1). The calculation is illustrated by equation B.2.

$$C_{Pu_{final}} = \frac{M_{Pu}}{V_0} \quad \text{(B.2)}$$

To calculate the uncertainty in the expected concentration, the variance in $C_{Pu_{final}}$ ($V_{C_{Pu_{final}}}$) is initially calculated using equation B.3,

$$V_{C_{Pu_{final}}} = \left(\frac{\partial C_{Pu_{final}}}{\partial M_{Pu}}\right)^2 V_{M_{Pu}} + \left(\frac{\partial C_{Pu_{final}}}{\partial V_0}\right)^2 V_{V_0} \quad \text{(B.3)}$$

where $V_{M_{Pu}}$ and V_{V_0} are the variances in the mass of metal and the initial volume of solution used in the experiment. The one sigma uncertainty ($s_{C_{Pu_{final}}}$) is subsequently calculated from equation B.4.

$$s_{C_{Pu_{final}}} = \sqrt{\left(\frac{1}{V_0}\right)^2 V_{M_{Pu}} + \left(-\frac{M_{Pu}}{V_0^2}\right)^2 V_{V_0}} \quad \text{(B.4)}$$

The uncertainties in the Pu concentrations calculated from the metal masses and initial volume of solution were based on a 1% relative standard deviation in each of the measurements. The uncertainties are given in Table 3-1.

Mass of Pu/Am Metal Dissolved

To calculate the amount of Pu and Am metal dissolved as a function of time, the estimated solution volume (Table B-20 and Table B-21) and the corrected Pu and Am concentrations (Table B-22 and Table B-23) at each sample time were used to calculate the mass of Pu and Am in solution. The calculated mass was expressed as a percentage of the total mass dissolved based on the maximum mass of Pu and Am in solution at the end of the experiment. The calculations are summarized in Table B-24 and Table B-25.

Table B-24. Actinide Metal Dissolved during Experiment M1

Sample ID	Dissolution Time (h)	Pu Mass Dissolved (g)	Am Mass Dissolved (mg)	Pu Dissolved (%)	Am Dissolved (%)
M1S1	0.25	0.322	1.71	8.53	10.21
M1S2	0.50	1.63	7.74	43.1	46.1
M1S3	0.75	2.22	10.1	58.8	60.2
M1S4	1.00	2.83	13.0	74.9	77.3
M1S5	1.25	3.72	16.4	98.3	98.0
M1S6	1.50	3.78	16.8	100	100
M1S7	1.75	3.52	16.3	93.2	96.9

Table B-25. Actinide Metal Dissolved during Experiment M2

Sample ID	Dissolution Time (h)	Pu Mass Dissolved (g)	Am Mass Dissolved (mg)	Pu Dissolved (%)	Am Dissolved (%)
M2S1	0.25	0.980	4.70	24.5	25.1
M2S2	0.50	1.74	7.87	43.6	42.1
M2S3	0.75	2.42	11.4	60.6	60.8
M2S4	1.00	2.93	14.6	73.2	78.0
M2S5	1.25	3.58	17.4	89.5	93.2
M2S6	1.50	3.94	18.7	98.4	100
M2S7	1.75	4.00	18.3	100	97.6

Uncertainties in the Masses of Pu and Am Metal Dissolved

The amounts of Pu and Am metal dissolved as a function of time were expressed as a percentage of the total mass dissolved based on the maximum mass of Pu and Am in solution (Table B-24 and Table B-25). This calculation is illustrated by equation B.5,

$$D(t) = \frac{M_{An(t)}}{M_{An(final)}}(100) \qquad (B.5)$$

where D(t) is the percentage of the actinide metal dissolved, $M_{An(t)}$ is the mass of the actinide in solution at time (t), and $M_{An(final)}$ is the maximum actinide mass in solution. To calculate the uncertainty in the percentage of the actinide metal dissolved, the variance in D(t) ($V_{D(t)}$) is initially calculated using equation B.6,

$$V_{D(t)} = \left(\frac{\partial D(t)}{\partial M_{An(t)}}\right)^2 V_{M_{An(t)}} + \left(\frac{\partial D(t)}{\partial M_{An(final)}}\right)^2 V_{M_{An(final)}} \qquad (B.6)$$

where $V_{M_{An(t)}}$ and $V_{M_{An(final)}}$ are the variances in the mass of the actinide in solution at time (t) and the maximum actinide mass in solution, respectively. The one sigma uncertainty ($s_{D(t)}$) is subsequently calculated from equation B.7.

$$s_{D(t)} = \sqrt{\left(\frac{100}{M_{An(final)}}\right)^2 V_{M_{An(t)}} + \left(-\frac{100M_{An(t)}}{M_{An(final)}^{\ 2}}\right)^2 V_{M_{An(final)}}} \qquad (B.7)$$

The uncertainties in the amount of Pu and Am metal dissolved as a function of time are given in Table B-26 and Table B-27for experiments M1 and M2, respectively.

Table B-26. Uncertainties in the Actinide Metal Dissolved during Experiment M1

Sample ID	Dissolution Time (h)	Pu Dissolved (%)	Am Dissolved (%)	Pu $S_{D(t)}$ (%)	Am $S_{D(t)}$ (%)
M1S1	0.25	8.53	10.21	0.66	0.72
M1S2	0.50	43.1	46.1	3.1	3.3
M1S3	0.75	58.8	60.2	4.2	4.3
M1S4	1.00	74.9	77.3	5.3	5.5
M1S5	1.25	98.3	98.0	7.0	6.9
M1S6	1.50	100	100	7	7
M1S7	1.75	93.2	96.9	6.6	6.8

Table B-27. Uncertainties in the Actinide Metal Dissolved during Experiment M2

Sample ID	Dissolution Time (h)	Pu Dissolved (%)	Am Dissolved (%)	Pu $S_{D(t)}$ (%)	Am $S_{D(t)}$ (%)
M2S1	0.25	24.5	25.1	1.76	1.78
M2S2	0.50	43.6	42.1	3.1	2.98
M2S3	0.75	60.6	60.8	4.3	4.3
M2S4	1.00	73.2	78.0	5.2	5.5
M2S5	1.25	89.5	93.2	6.3	6.6
M2S6	1.50	98.4	100	7	7
M2S7	1.75	100	97.6	7.1	6.9

Appendix C. Pu Metal Dissolution Rate

Dissolution Rate Data

The experimental data used to calculate the dissolution rate of the Pu metal coupons are presented in Table C-1 and Table C-2. The data include the mass, length, width, and thickness of the Pu metal as functions of the dissolution time. Calculations summarized in the tables include the surface area and mass to surface area ratios which are also functions of the cumulative dissolution time.

Table C-1. Dissolution Rate Data for Experiment M1

Dissolution Time (h)	Pu Metal Mass (g)	Pu Metal Length (mm)	Pu Metal Width (mm)	Pu Metal Thickness (mm)	Surface Area (cm^2)	Mass/Surface Area Ratio (mg/cm^2)
0.0	3.7826	34.63	11.62	0.93	8.908	424.6
0.25	3.0316	34.14	11.33	0.83	8.491	357.0
0.50	2.1801	33.37	11.20	0.47	7.894	276.2
0.75	1.5174	32.43	10.34	0.39	7.040	215.5
1.00	0.8440	32.29	10.15	0.24	6.759	124.9
1.25	0.2273	28.15	8.97	0.27	5.251	43.3

Table C-2. Dissolution Rate Data for Experiment M2

Dissolution Time (h)	Pu Metal Mass (g)	Pu Metal Length (mm)	Pu Metal Width (mm)	Pu Metal Thickness (mm)	Surface Area (cm^2)	Mass/Surface Area Ratio (mg/cm^2)
0.0	3.9524	27.50	14.62	0.92	8.816	448.3
0.25	3.1573	27.22	13.98	0.84	8.303	380.3
0.50	2.2992	26.99	14.07	0.48	7.989	287.8
0.75	1.6249	26.70	14.18	0.38	7.883	206.1
1.00	0.9019	26.50	13.87	0.20	7.513	120.1
1.25	0.2976	25.45	12.41	0.11	6.400	46.5

Appendix D. UV-Visible Spectra for Tests 1–6.

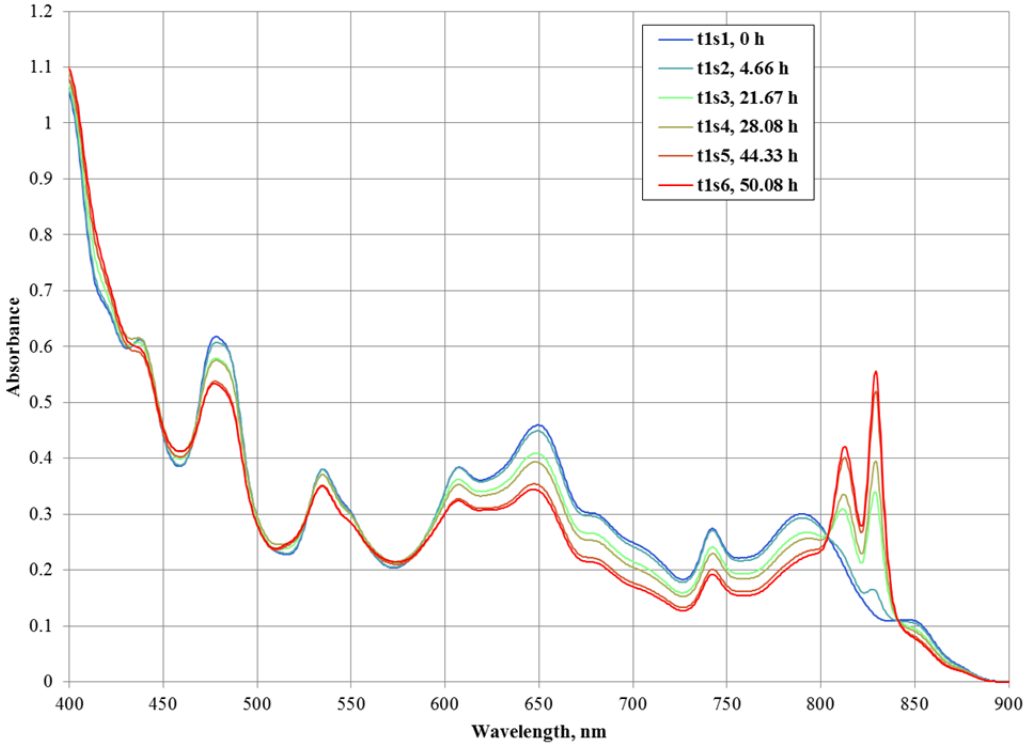

Figure D-1. Spectra of the simulated dissolver solution showing oxidation of Pu(IV) to Pu(VI) as a function of solution heating time for Test 1.

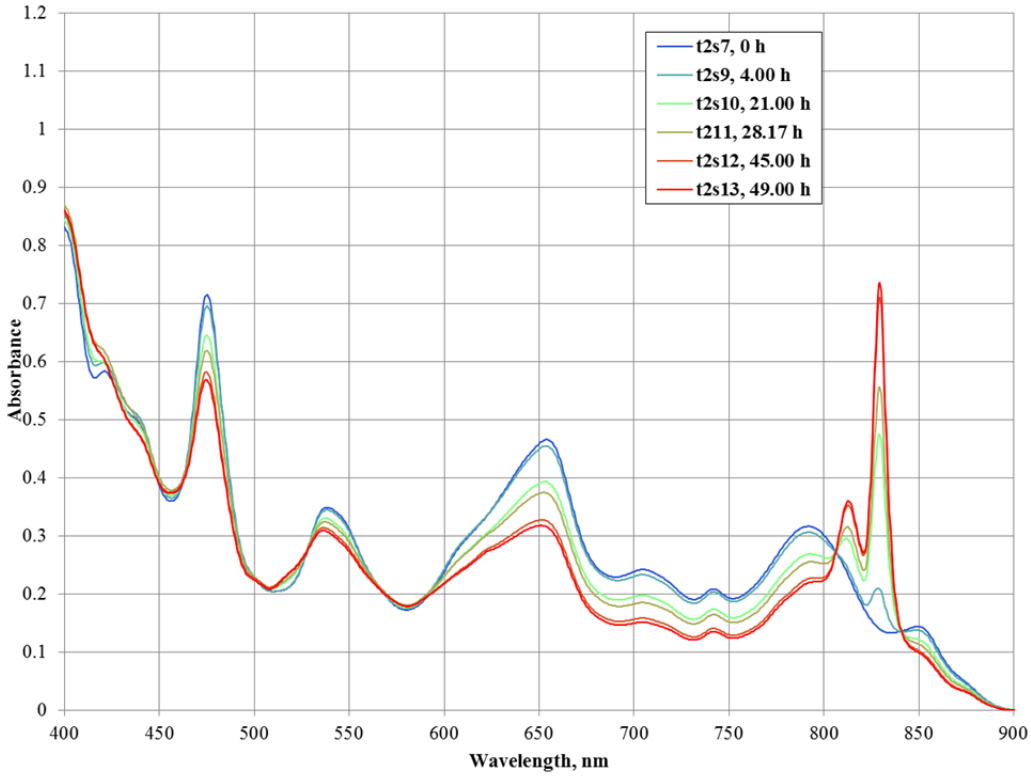

Figure D-2. Spectra of the simulated dissolver solution showing oxidation of Pu(IV) to Pu(VI) as a function of solution heating time for Test 2.

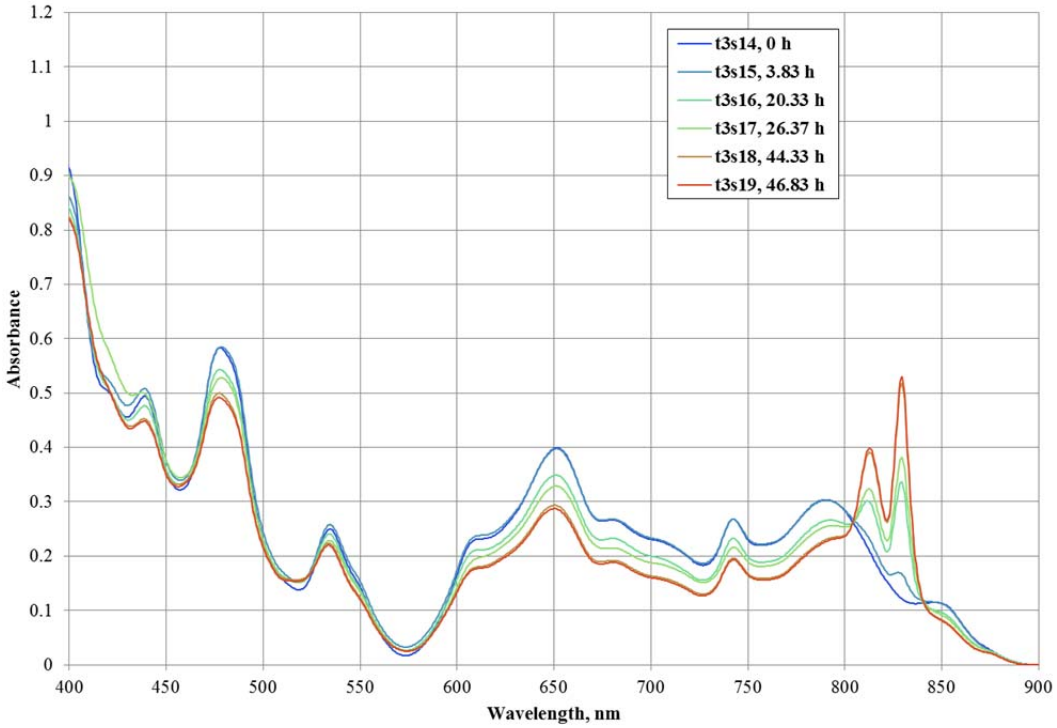

Figure D-3. Spectra of the simulated dissolver solution showing oxidation of Pu(IV) to Pu(VI) as a function of solution heating time for Test 3.

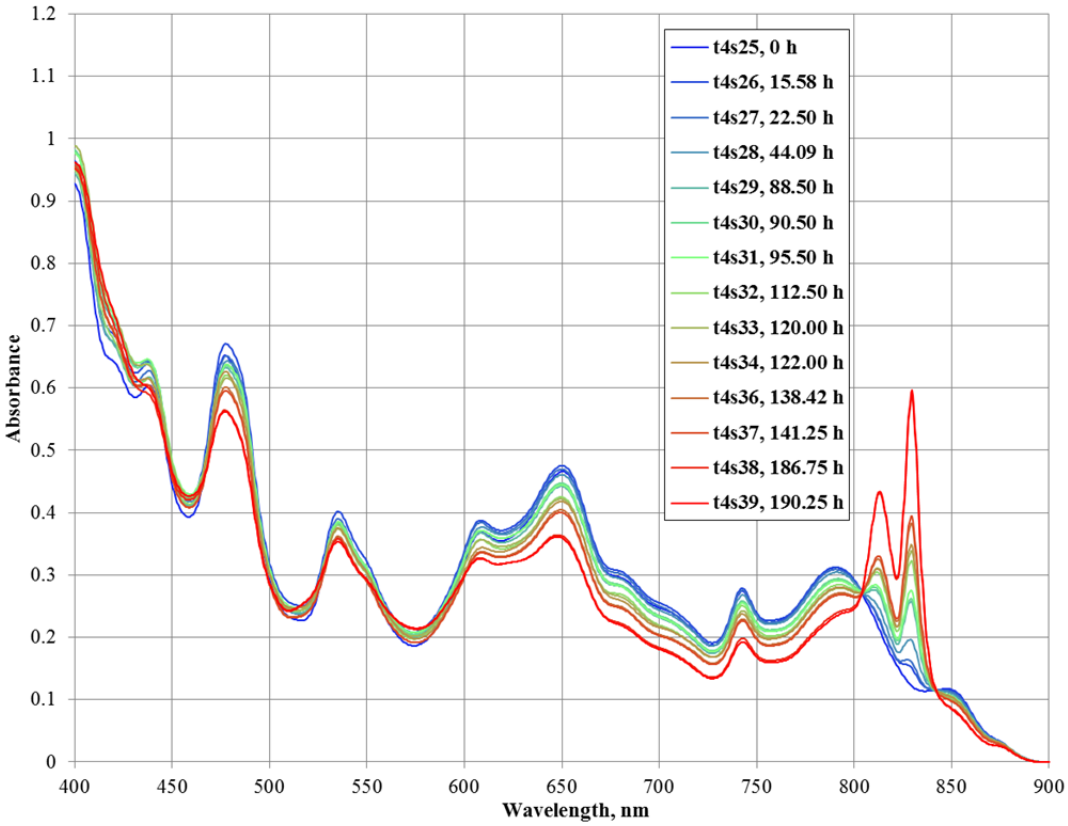

Figure D-4. Spectra of the simulated dissolver solution showing oxidation of Pu(IV) to Pu(VI) as a function of solution heating time for Test 4.

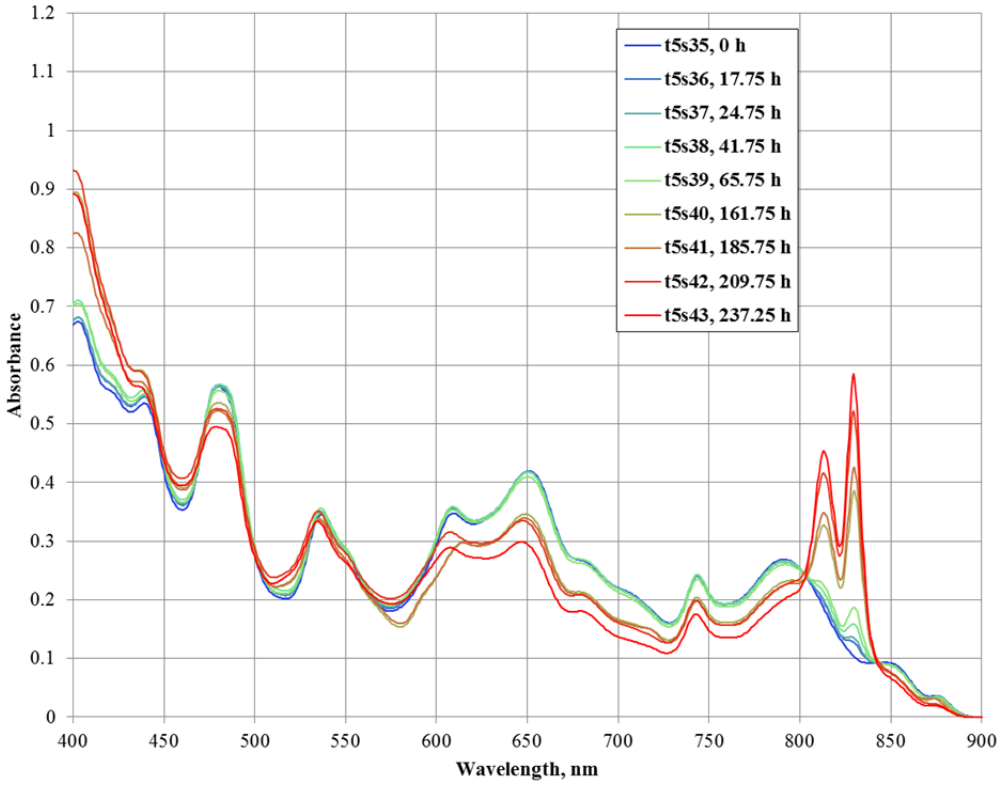

Figure D-5. Spectra of the simulated dissolver solution showing oxidation of Pu(IV) to Pu(VI) as a function of solution heating time for Test 5.

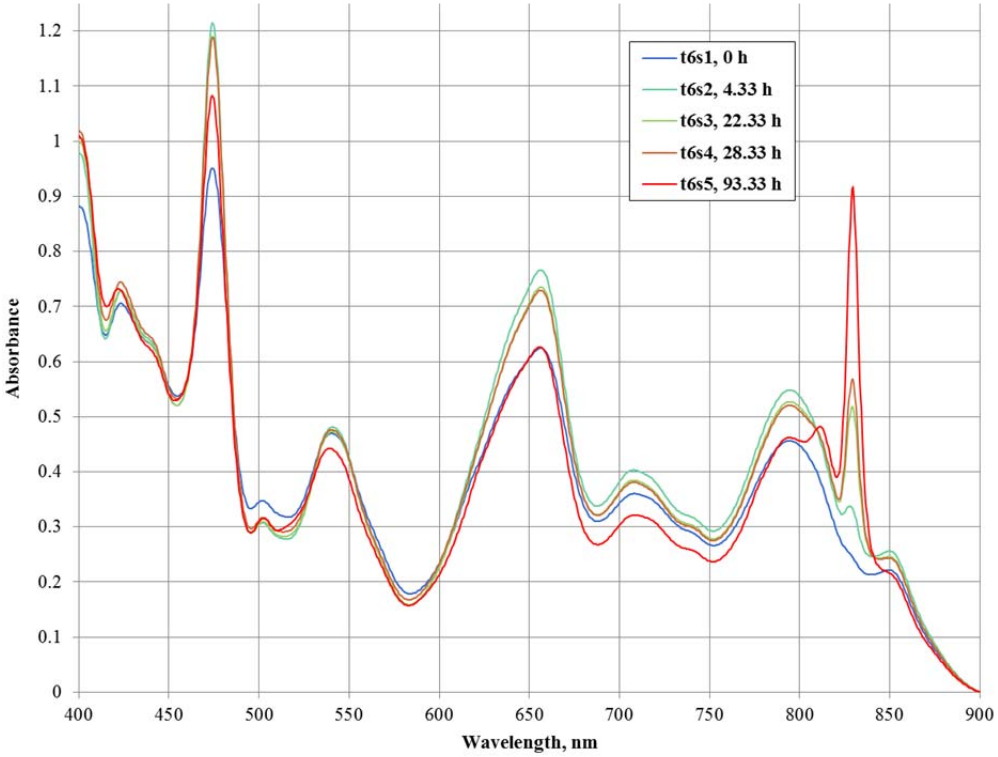

Figure D-6. Spectra of the simulated dissolver solution showing oxidation of Pu(IV) to Pu(VI) as a function of solution heating time for Test 6.

Distribution:

S. L. Marra, 773-A
T. B. Brown, 773-A
D. H. McGuire, 999-W
S. D. Fink, 773-A
C. C. Herman, 773-A
E. N. Hoffman, 999-W
F. M. Pennebaker, 773-42A
W. R. Wilmarth, 773-A
W. E. Harris, 704-2H
J. B. Schaade, 704-2H
P. B. Andrews, 704-2H
M. Lewczyk, 221-H
K. P. Burrows, 704-2H
K. J. Gallahue, 221-H
J. E. Therrell, 704-2H
K. J. Usher, 704-2H
S. L. Hudlow, 221-H
W. H. Clifton, Jr. 704-2H
S. L. Garrison, 704-2H
K. P. Crapse, 773-A
E. A. Kyser, 773-A
T. S. Rudisill, 773-A
R. A. Pierce, 773-A
J. M. Duffey, 773-A
K. M. Taylor-Pashow, 773-A
M. C. Thompson, 773-A
P. E. O'Rourke, 773-A
R. J. Lascola, 773-41A
L. T. Sexton, 773-42A
P. R. Jackson, 703-46A

Records Administration (EDWS)